Effect of Operation Conditions on Membrane Distillation Performance for Recovery the Valuable Compounds from Food Wastewater

Sothyreak Chhun

A Thesis Submitted in Fulfillment of the Requirements for the Degree of

Master of Engineering in Environmental Engineering

Prince of Songkla University

2015

Effect of Operation Conditions on Membrane Distillation Performance for Recovery the Valuable Compounds from Food Wastewater

Sothyreak Chhun

A Thesis Submitted in Fulfillment of the Requirements for the Degree of

Master of Engineering in Environmental Engineering

Prince of Songkla University

2015

Thesis Title	Effect of Operation Conditions on Membrane Distillation Performance for Recovery the Valuable Compounds from Food Wastewater
Author	Miss. Sothyreak Chhun
Major Program	Master of Engineering program in Environmental Engineering

---

Major Advisor

…….
(Dr. Watsa Khongnakorn)

Co-advisor

……
(Assoc. Prof. Dr. Wirote Youravong)

Examining Committee:

……..…….Chairperson
(Asst. Prof. Dr. Chaisri Suksaroj)

……..…Committee
(Assoc. Prof. Dr. Apichat Boontawan)

……..…….…….Committee
(Asst. Prof. Dr. Charongpun Musikavong)

……...…….Committee
(Dr. Watsa Khongnakorn)

…….Committee
(Assoc. Prof. Dr. Wirote Youravong)

The Graduate School, Prince of Songkla University, has approved this thesis as fulfillment of the requirements for the Master of Engineering Degree in Environmental Engineering.

…..……
(Assoc. Prof. Dr. Teerapol Srichana)
Dean of Graduate School

This is to certify that the work here submitted is the result of the candidate's own investigations. Due acknowledgement has been made of any assistance received.

...……Signature

(Dr. Watsa Khongnakorn)
Major Advisor

……..……...…Signature

(Miss. Sothyreak Chhun)
Candidate

I hereby certify that this work has not been accepted in substance for any degree, and is not being currently submitted in candidature for any degree.

…...…….Signature

(Miss. Sothyreak Chhun)
Candidate

Thesis Title	Effect of Operation Conditions on Membrane Distillation Performance for Recovery the Valuable Compounds from Food Wastewater
Author	Miss. Sothyreak Chhun
Major Program	Master of Engineering program in Environmental Engineering
Academic Year	2014

ABSTRACT

Membrane distillation (MD) is a relatively new process that is being investigated worldwide as a low cost, energy saving compared to conventional separation processes. The experiments were carried out in co-current mode of outside-in with feed temperature in range from 40 °C to 70 °C and kept constant at 20 °C in permeate side. The flow rate also varied from 500 ml/min to 1500 ml/min at the feed side and kept constant at 500 ml/min which the Reynolds number in range from 900 to 4,346. The study was performed with synthesis solution to obtain optimum condition before generate with real wastewater. The optimum condition was found at feed temperature of 70 °C under the operating condition with 1000 l/min of feed flow rate. As the results, the permeate flux obtained were 13.8 kg/m².h, 13.9 kg/m².h and 12.1 kg/m².h of the 3.5 wt.% of NaCl, 5 wt.% of sucrose, and 0.04 wt.% of BSA, respectively. Similarity, the real wastewater was also applied with the optimum condition. In results, the permeate flux obtained were 12.7 kg/m².h, 10.5 kg/m².h, and 5.6 kg/m².h for brine solution, tofu whey, and tuna cooking juice, respectively. In DCMD process, it is very effective in removing the COD from the wastewater reached 98 %, which enable to discharge free to water source or recycling used. Moreover, 26.21 % of sucrose was recovered from tofu whey and 32.53 % of protein was recovered from tuna cooking juice. Moreover, the study found that the highest gain output ratio (GOR) was obtained at feed temperature of 60 °C, which have significant influence on DCMD process to reduce energy consumption.

ACKNOWLEDGEMENT

Firstly, I would like to express my sincere thanks to my advisor and co-advisor, not for their guidance, inspiration, support and encouragement in every stage of my Master study, but also for providing me with an excellent atmosphere and giving me trust and confident to carry out the research.

I am so grateful to Membrane Science and Technology Research Center for providing me to conduct my experiments and all of laboratory facilities.

I am so thankful to Thai Higher Education Institute and Austria government through the ASEA-UNINET Thailand on place for supporting my International Master Research scholarship program.

I also would like to thank Kurita Water and Environment Foundation for the Research Grants 2013.

Next, I am thankful to many friends who helped, encouraged, motivated during the study. I have gained a new perspective which is quite different from what I learnt during my previous undergraduate. Especially I thank to my lab mate for helping me to collect the samples and teaching my Thai language during my stay in Thailand. My appreciation forward to many friends and Thai undergraduate students and various international friends for all their help, encourage and friendship.

Finally, I would like to thank my parents who nourished me and made me what I am today and also sisters and relatives and friends in Cambodia for encouraging me to go overseas to pursue a degree.

Sothyreak Chhun

CONTENTS

Page

LIST OF TABLES

Page

LIST OF FIGURES

Page

LISTS OF ABBREVIATIONS AND SYMBOLS

h_f : Feed-side local heat-transfer coefficient($W/m^2.K$)

h_p : Permeate-side local heat-transfer coefficient ($W/m^2.K$)

TPC : Temperature polarization coefficient

T_f : Feed side bulk temperature (K)

T_{fm} : Feed side membrane surface temperature (K)

T_p : Permeate side bulk temperature (K)

T_{pm} : Permeate/distillate side membrane surface temperature (K)

C_p : Specific heat (J/kg.K)

J : Mass flux through the membrane ($kg/m^2.s$)

k_m : Thermal conductivity of the membrane (W/m.K)

k_g : Thermal conductivity of the air (W/m.K)

k_s : Thermal conductivity of the solid phase of themembrane (W/m.K)

K : Solute mass transfer coefficient (m/s)

Nu : Nusselt number (dimensionless)

Pr : Prandtl number (dimensionless)

Q : Heat flux (W/m^2)

T : Temperature (K)

H_v : Latent heat of vaporization (J/kg)

CPC : Concentration polarization coefficient (dimensionless)

C_{mf} : Concentration of membrane

C_{bf} : Concentration of feed side

EE : Evaporation efficiency (%)

Sh : Sherwood number (dimensionless)

Sc : Schmidt number (dimensionless)

d_h : Hydraulic diameter of channel (m)

D : Diffusion coefficient of solute (m^2/s)

v : Velocity (m/s)

LISTS OF ABBREVIATIONS AND SYMBOLS

Greek symbols

δ	: Membrane thickness (m)
ε	: Porosity (%)
μ	: Liquid viscosity (Pa/s)
ρ	: Liquid density (kg/m^3)

Chapter 1
Introduction

1.1 Background and rational

Nowadays, as the world economy growth so rapidly, industries in all sectors are also increasing at significant speed especially in the food and beverage. Thailand is the largest canned tuna products exporter in the world. More than 224,558 tons of canning tuna are produced annually [1]. During canned tuna processing, there are many aqueous effluents such as washing, rinsing and cooking. In the cooking process, 1 ton of raw material consumes approximately 0.5 m^3 of water, which generated about 0.768 m^3 of wastewater [2]. Hsu et al [3] indicated that in tuna cooking juices contain proteins approximately 4% soluble protein, 35% of liquid waste. Adler-Nissen [4] has used an enzymatic modification of food protein which has improved the palatability and storage stability of protein source from tuna cooking juice. Moreover, application of protein hydrolysate from tuna cooking juice for animal food ingredient has increased dramatically [4-8]. Beside this, tofu whey is the liquid which drain out of tofu making is one of the other food wastewater contained oligosaccharide and mostly is stachyose and raffinose. Due to their valuable compounds, some researchers have found many applications to recover such by-products to use as an ingredient in the food industry.

In food processing above, the environmental concern is the use of a large amount of fresh water for processing, raw material washing and products. The wastewater generated by these food processing factories is rich of high loaded of organic and inorganic.

Recently, membrane distillation (MD) has been alternative technology separation process with promising in desalination and food industry. MD has been used for concentrated of fruit juice [9, 10], sugar syrup [11] and whey protein [12, 13]. The advantages of MD compared to other separation process are followed:

(1) Lower operating temperatures than which applied in conventional distillation. The process performed at feed temperature is lower than the boiling point

of water. Moreover, alternative energy such as solar, industrial waste heat and desalination waste heat can be employed to the feed side.

(2) Lower operating pressures than other membrane process, the operating pressure generally near the atmospheric pressure.

(3) High rejection close to 100 % (in theoretical) of ionic, macromolecules, colloids and other non-volatiles.

In addition, MD process is using the different temperature gradient to operate the system. Meanwhile, the wastewater temperature from the food factory is about 60 to 80 °C. Therefore, it can save energy consumption by using waste heat as a gradient temperature. MD process is one of the most suitable process uses for wastewater recovery and produces the highly purified quality of water and by-product such as protein, sugar, oligosaccharide [14]. Therefore, this research is focuses on the recovery of valuable compounds from tuna cooking juices and tofu whey that reduces the COD in the effluent, the footprint of wastewater treatment plant. The product and can be use as the alternative for healthy food as high protein content using the new technology which consumes less energy [15, 16].

1.2 Review of literature

1.2.1 General

In this work, three synthesis solutions of sodium chloride, sucrose, and bovine serum albumin (BSA) are used to study the mechanism of membrane in the system which could be implied to the real wastewater of brine solution, tofu whey, and tuna cooking juice.

1.2.2 Characteristics overall of wastewaters

1.2.2.1 Brine solution

In terms of wastewater treatment, brine waste is the highly concentrated by-product that results from treating blackish water, seawater, or the effluent from the reverse osmosis process in the industrial [17-19]. Brine waste contains both moderate to high concentration of organic and inorganic compounds. The organic compounds exist in RO brine mostly consists of slow-and hard-to-degrade organic consistent [20].

Brine waste also contains high salt concentration and total dissolved solids (TDS) concentration which normally higher than 2,000 ppm [19].

High salt concentration has an involving effect on the human health of directly contaminated area since most of industrial waste discharge instantly to the river or water source. The lack of waste treatment, salinity acts as a stressor on the environment. According to the broad definition of an environmental risk assessment (ERA), an unnaturally high amount of salinity can be considered a toxin [21].

The characteristics of brine wastewater as present in Table 1.1.

Table 1.1 Characteristics of brine waste

Raw material	pH	TOC (mg/l)	TDS (mg/l)	Sodium (mg/l)	Chloride (mg/l)	References
Brine wastewater	6.82	-	21,326	2,759	6,442	[22]
	-	111	945	-	-	[20]
	-	-	105,000	29,320	-	[23]
	8.8	-	49,800	28,600	51,800	[24]

1.2.2.2 Tofu whey

Tofu whey is the liquid which drained out during making tofu and it is considered as wastewater and discharged into a water source which causes many problems to the environment. According to researches, tofu whey contains much of nutrition such as proteins, fat, salt, carbohydrate, and oligosaccharides are being a crucial source of food ingredient [25, 26].

The details of the basic steps of the tofu- making process are as follows [27, 28]:

- *Soaking*: Soaked the dry soybeans in water overnight or at least up to 16 hours. Normally the volume of water is about 2-3 times of the bean volume.
- *Draining and washing*: The soaked beans are drained and washing with fresh water 2-3 times.
- *Grinding*: Grind the soybeans in the batches with their soaking water in a food processor/blender until the beans ground fine. The slurry is collected in a large pot.
- *Filtering*: The bean slurry is filtered through the cheesecloth, or pressing sack. Carefully gather up the sides of the cheesecloth and twist it as much as soy milk possible. The residue, known as soy pulp or Okara is removed.

- *Cooking*: The soy milk is heated to the boiling and maintained at this temperature for 5-10 min. Right after using the wooden spoon stirred the soy milk to prevent sticking.
- *Coagulating*: After soy milk is heated, a coagulant suspension is prepared by mixing a powder coagulant with some hot water. The most commonly coagulant used is calcium sulfate; magnesium chloride and as well as lemon juice are recommended. After coagulant is added, the mixture is allowed to stand for about 20-30 min for coagulation to complete. However, the texture of soybean curd was different depending on the types of coagulant is used.
- *Molding*: The soy curd is ready to transfer in the forming box with the cheesecloth. Meanwhile pressed out, the tofu whey is drained out for sampling and the tofu curd become firm. Cooled the tofu and cut into cakes, which ready to be served.

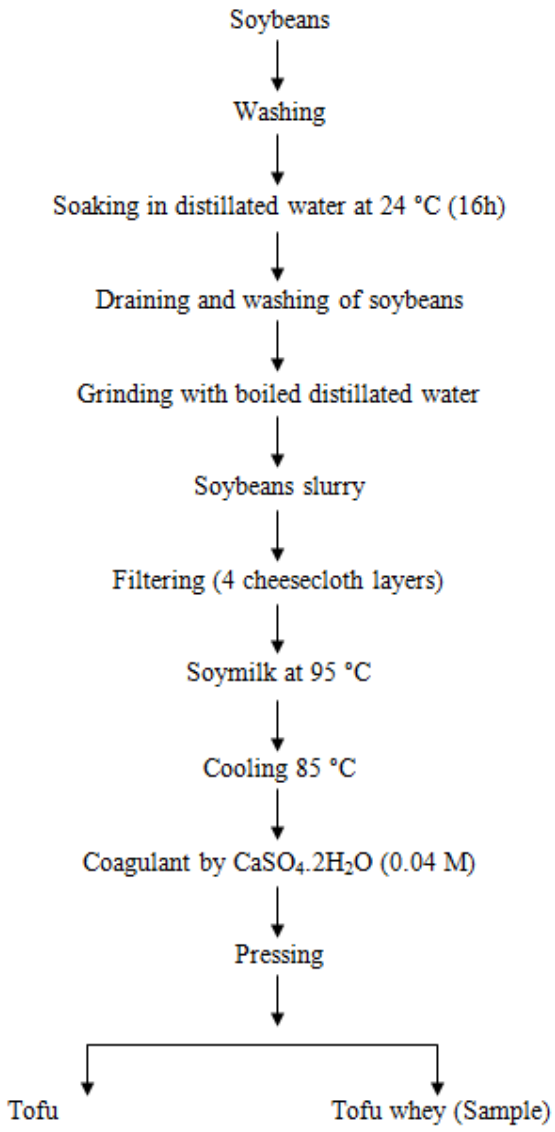

Figure 1.1 Flow chart of making tofu [29]

- The utilization of tofu whey by-products

Nowadays, a by-product of tofu whey is more seen as a potential resource instead of waste. Optimal utilization of these products is becoming an increasingly major ingredient to supply more raw materials for various purposes. Large amounts of protein and oligosaccharide rich in tofu whey are discharged without any attempt of recovery. According to some researches, tofu whey contains oligosaccharides which mostly are stachyose, raffinose and as well as proteins are nutritional components to produce a new ingredient of functional food and drug [30-32].

The characteristics of tofu whey wasted are presented in Table 1.2.

Table 1.2 Characteristics of tofu whey wastewater

Compositions	pH	TSS (mg/l)	TOC (mg/l)	BOD (mg/l)	COD (mg/l)	Sucrose (mg/l)	Protein (mg/l)	Ref
Tofu whey wastewater	3.6	936	-	8,852	29,700	-	-	[33]
	-	-	8,810	9,800	27,440	800	630	[34]
	-	-	-	-	-	39,800	3,490	[35]
	4.27	-	-	-	46,300	-	-	[36]
	5	4,550	-	-	-	1,400	-	[37]

1.2.2.3 Tuna cooking juice

Thailand is the largest canned tuna products exporters in the world. More than 224,558 tons of canned tuna have produced annually [1]. During canned tuna processing, there are 25 to 30% solid waste (e.g., head, skin, viscera) and about 35% liquid waste (e.g., blood, tuna cooking juice and oil) were produced [38]. In Figure 1.2 shows the flow chart of tuna canned process and wastewater tuna canned process.

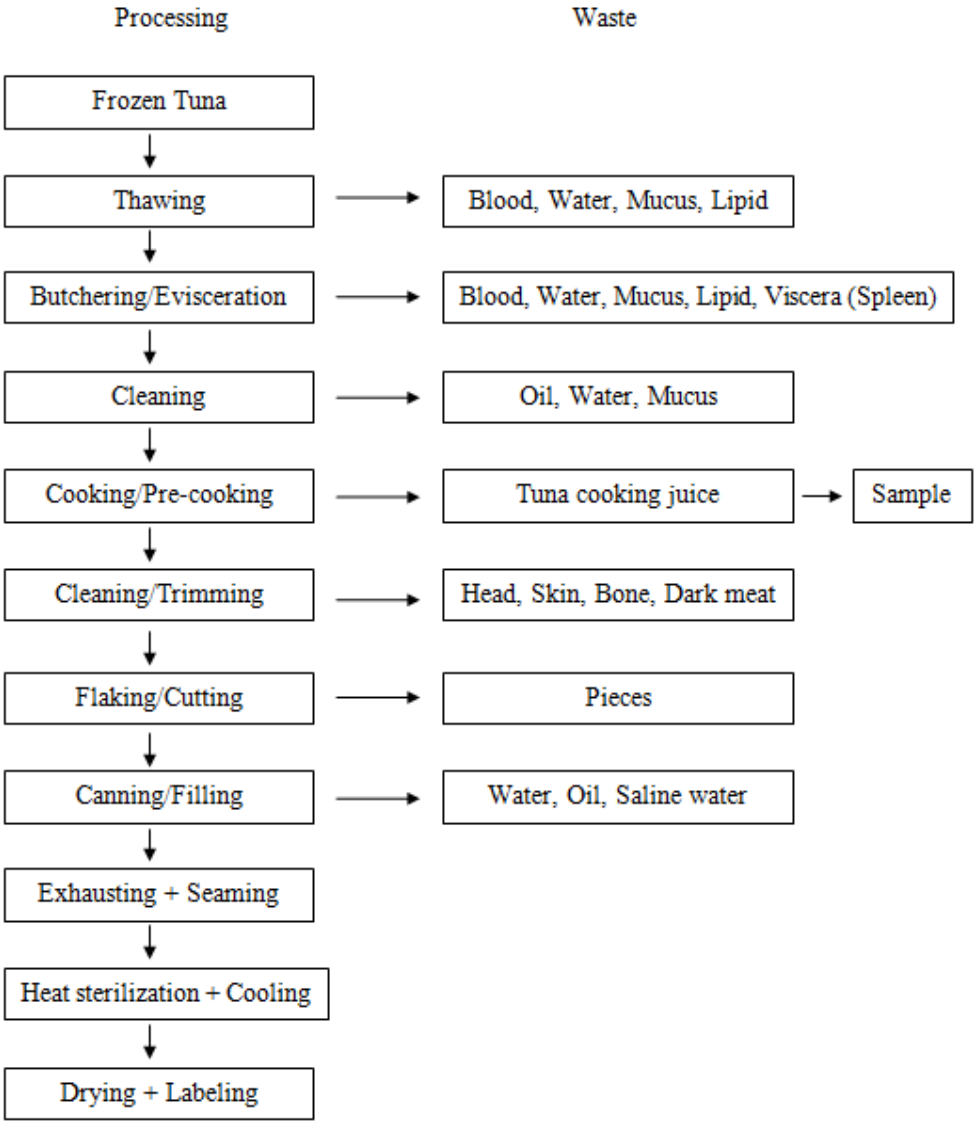

Figure 1.2 Typical of flow chart for tuna canning process [39]

The tuna cooking juice come from tuna cooking processing to remove the sarcoplasmic proteins (SP) and gelatin [40]. In tuna cooking juice has a very high organic loading of COD and contained about 25-30% liquid waste (e.g. blood, tuna cooking juice, oil), about 35-40% solid waste (e.g. head, skin, viscera) and protein source [41]. According to several researches, the characteristics of tuna cooking juice as shown in Table 1.3.

Table 1.3 Characteristics of tuna cooking juice [30]

Raw material	pH	COD (mg/l)	Protein (%)	Total solid (mg/l)	Salt (%)	Fat (%)	Reference
Tuna cooking juice	5.91	19,000	3.15	-	-	-	[42]
	6.09	52,416	4.9	81,503	0.22	1.89	[43]
	6.07	49,476	5.5	82,800	0.36	0.17	[44]
	6.07	73,617	4.15	68,450	-	-	[45]
	6.48	-	5.63	73,200	0.7	0.04	[46]

1.2.3 Membrane distillation

Membrane distillation (MD) is the membrane process which utilizes porous, hydrophobic membrane. The vapor pressure different between feed and permeate side act in role as the driving forces which is resulting from different temperature of the feed and permeate side. The vapor pressure, which is across the membrane was condense at the permeate side. The hydrophobic membrane admits only water vapor across the membrane with temperature not exceed to the boiling point.

1.2.3.1 Type of membrane

Hydrophobic and micro-porous membrane is applied in the MD process. In general, micro-porous hydrophobic membrane makes from different type polymers such as polyvinylidene fluoride (PVDF), polytettra flourethylene (PTFE),

polyethylene (PE) and polypropylene (PP). Among of them, PTFE membrane is the most hydrophobic ones showed outstanding thermal stability and chemical resistance. Otherwise, PTFE membrane is the most expensive, while as PVDF membrane exhibits good thermal and chemical resistance. There are two types membrane module used in MD flat sheet and hollow fiber. Membrane thickness is a significant characteristic in MD process in the range from 50-250 μm [47, 48]. To obtain a high permeate flux, the membrane thickness must be as thin as possible. In contrast, to achieve better heat efficiency the membrane thickness should be as thick as possible. Laganà et al., (2000) [49] suggested that the optimum membrane thickness should be in the range 30-60 μm.

1.2.3.2 Porosity (ε)

Membrane porosity refers to the void volume of the membrane. Membrane with higher porosity could be achieved greater surface area for evaporation and lower conductive heat loss. Normally, the MD membrane porosity varied between 30-85 %. The porosity (ε) can be determined by the Smolder-Franken equation

$$\varepsilon = 1 - \frac{\rho_m}{\rho_{pol}} \tag{1.1}$$

Where ε: Porosity (%), ρ_m: Density membrane (kg/m³), ρ_{pol}: Density polymer material (kg/m³).

1.2.3.3 Pore size (Ø)

The membrane used in MD indicated pore sizes ranging 0.1 μm to 1 μm [50]. The flux permeates increase with increasing pore size. However, in order to avoid the pore wettability, small pore size should be selecting [51].

1.2.3.4 Thermal conductivity (k)

The thermal conductivity of the membrane should be small in order to reduce the heat loss through the membrane from the feed side to permeate side. The conductive heat loss is inversely proportional to the membrane thickness. However, the selection the thicker of membrane will decrease flux permeability. The thermal conductivities generally vary in the range 0.15-0.45 W/m.K [47].

1.2.3.5 Contact angle (θ)

The contact angle is a common measurement of the hydrophobic or hydrophilic behaviors of a material. The contact angle is related to the pore wettability. The value of contact angle greater than 90^o, the material considered hydrophobic. Otherwise, if it less than 90^o the material considered hydrophilic [50].

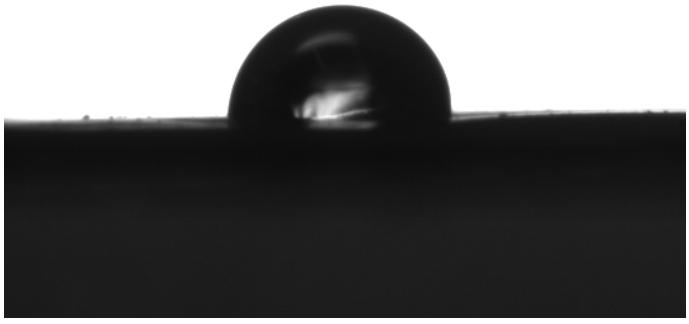

Figure 1.3 Contact angle of PVDF membrane [This work]

1.2.3.6 Membrane wetting (LEP)

Membrane distillation can take place whenever the membrane remains in the dry, which allow only water vapor, go through the membrane. Liquid entry pressure (LEP) is the minimum pressure that will be employed onto feed solution before overcoming the hydrophobic forces of the membrane and penetrate to the

membrane pore size. LEP is the characteristic of each membrane and allows preventing wetting of the membrane pore. LEP is correlated to liquid surface tension, contact angle of liquid on the membrane surface, and the shape and size pore of the membrane. LEP can be express as shown in Eq (1.2). Garcı et al., (2000) [52] revealed that the LEP could be 200-400 kPa for the membrane pore size of approximately to 0.2μm, while its as low as 100 kPa for membrane with pore size 0.45 μm. Kullab & Martin., (2011) [53] indicated that fouling not only ceases to pore clogging in MD membrane which reduced the effective area of permeate flux, but also lead the pressure drop which exceeds to LEP that could make the membrane partial wetting.

$$LEP = -\frac{2\gamma B\cos\theta}{R} \qquad (1.2)$$

Where γ is surface tension of water (N/m), B is geometric factor (dimensionless), R is pore radius (μm), and θ is contact angle (°).

1.2.3.7 Configurations of membrane distillation

Membrane distillation is divided to 4 different configurations are (a) Direct contact membrane distillation (DCMD), (b) Vacuum membrane distillation, (c) Air gap membrane distillation (AGMD), (d) Sweeping gas membrane distillation (GSMD).

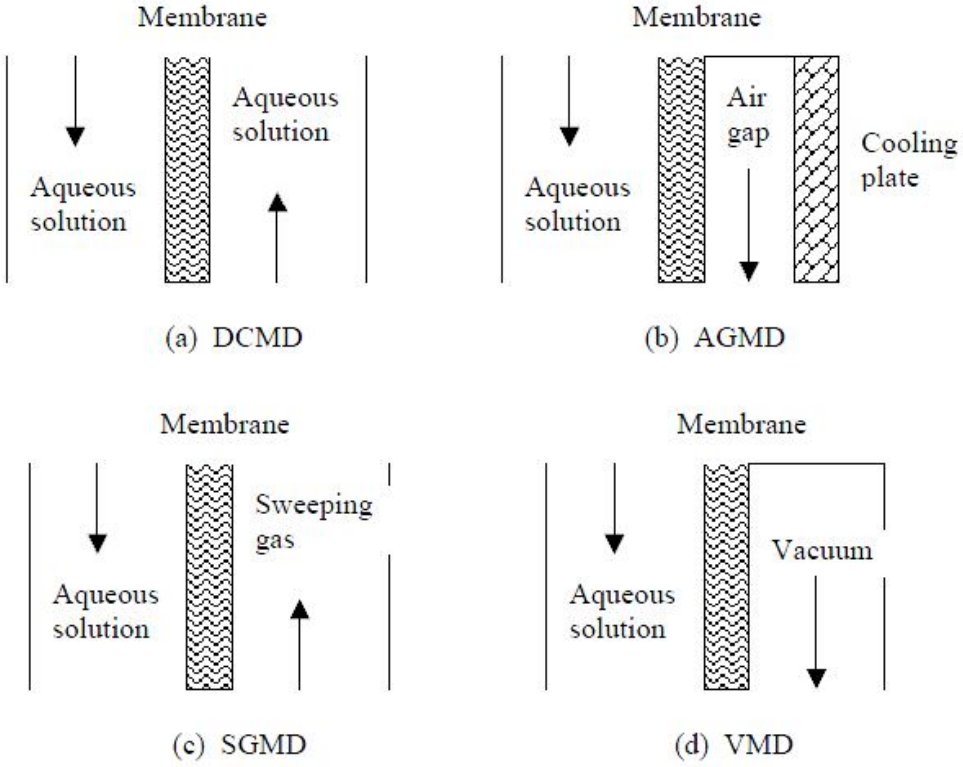

Figure 1.4 Different types of MD Configurations [54]

- Direct contact membrane distillation (DCMD)

Direct contact membrane distillation (DCMD), in which the membrane is in direct contact with liquid phases. This is the simplest configuration capable of producing reasonably high flux. It is best suited for applications such as desalination and concentration of aqueous solutions (e.g., juice concentrates) [1, 55-59].

- Sweeping gas membrane distillation (SGMD)

Sweep gas membrane distillation (SGMD), in which stripping gas is used as a carrier for the produced vapor. It is used when volatiles are removed from an aqueous solution [60-64].

- Air gap membrane distillation (AGMD)

Air gap membrane distillation (AGMD), in which an air gap is interposed between the membrane and a condensation surface. The configuration has the highest energy efficiency, but the flux obtained is generally low. The air gap configuration can be widely employed for most membrane distillation applications [65], particularly where energy availability is low.

- Vacuum membrane distillation (VMD)

Vacuum membrane distillation (VMD), in which the permeate side is vapor or air under reduced pressure, and if needed, permeate is condensed in a separate device. This configuration is useful when volatiles are being removed from an aqueous solution [66, 67].

Table 1.4 Summary of the area where MD process were successfully applied on laboratory scale [51]

Application area	MD			
	DCMD	VMD	SGMD	AGMD
- Desalination and pure water production from blackish water	√	√	√	√
- Textile industry (removal of dyes and wastewater treatment)	√	√		
- Chemical industry (concentration of acids or removal of VOCs from water)	√	√	√	√
- Pharmaceutical and biochemical industries (removal of water from blood and proteins solution, wastewater treatment)	√			
- Food industry (wastewater treatment and concentration juice or milk)	√	√		√
- Nuclear industry (concentration of radioactive solution and wastewater treatment, pure water production)	√			

1.2.4 Operation condition on Performance of DCMD

The key parameters that affect on performance or flux obtain:

1.2.4.1 Temperature

As we know that, temperature is important factor which affect to the permeate flux. During the temperature is the driving force increase the transmembrane vapor pressure also increase, which the increasing permeate flux. It was found that the flux was increased more than 2 LMH for every 1°C in the feed solution [68]. At the same time, the temperature variation should be precaution in separating process in order to avoid denaturing or destroy the sample such protein compounds.

1.2.4.2 Cross flow velocity

To reduce the temperature and concentration polarization effects, the feed and permeate flow rates must be increased. When the flow rate is increased the temperature and non-volatile solute concentration at the membrane surface become closer to the corresponding bulk temperature and bulk concentration. However, the flow rate should be investigated in order to avoid membrane pore wetting [69].

1.2.4.3 Concentration

Concentration also one of among factor that could affect to the permeate flux. During increasing of the non-volatile concentration in the feed solution, the results in reduction of permeate flux [69].

The Experiment flow was designed by outside-in of the membrane in the module. The Reynolds numbers of the feed and the distillate flowing through the shell and tube side were defined as the diameter-based Reynolds number (*Re*). The Reynolds number is normally defined in the following way:

$$Re = \frac{d_h v \rho}{\mu} \tag{1.3}$$

Where *Re* is the Reynolds number, d_h is the hydraulic diameter, v is the velocity, ρ is the water density, and μ is the dynamic viscosity.

In the calculation of Reynolds number based on eq. (1.3), i.d of fiber (d_i) and linear velocity are used for the lumen side parallel flow, and o.d of fiber (d_o) and interstitial velocity are used for the shell side cross-flow.

$$Interstitial\ velocity = \frac{\text{Feed flow rate}}{\text{Open area for flow through the shell side}} \quad (1.4)$$

$$Linear\ velocity = \frac{\text{Distillate flow rate}}{\text{Open area for flow through the lumen side}} \quad (1.5)$$

Thus, open area for flow through the shell side = $\pi/4(d_{o.m}^2 - d_o^2)$, open area for flow through lumen side = $n\pi\ (d_i^2/4)$.
Where $d_{m.o}$ is the outer diameter of module, d_o is the outer diameter of fiber, d_i is the inner diameter of fiber.

1.2.5 Permeate flux

In the membrane distillation (MD) process water evaporates through the non-wetted membrane pores. The driving force for the mass transfer is expressed by the vapor pressure difference across the membrane caused by the exit temperatures and the compositions of the layers of the membrane. Permeate flux can be expressed as Eq. (1.6)

$$J = \frac{\Delta W}{A.\Delta T} \quad (1.6)$$

Where J is the permeate flux ($kg/m^2.h$), ΔW is the quantity of distillate (kg), A is the inner surface area of the hollow fiber membrane (m^2), and ΔT is the interval time (h).

1.2.6 Recovery efficiency

The effectiveness of the process was confirmed by how much of solution in feed material is achieved during operation. This expected would be present by using Equation (1.7) and (1.8) as following.

Percent recovery

$$R_{recovery} = \frac{(C_i - C_f)}{C_b} \times 100 \quad (1.7)$$

Where C_i is the initial concentration, C_f is the final concentration

Percent rejection

$$R_{rejection} = \frac{(C_f - C_p)}{C_f} \times 100 \quad (1.8)$$

Where C_f is the feed concentration, C_p is the permeate concentration

1.2.7 Heat transfer in DCMD

In MD process, heat transfer divided into three regions which show in Figure 1.5 such as (1) heat transfer through boundary layer of feed solution, (2) heat transfer through membrane pore, and (3) heat transfer through boundary layer of permeate.

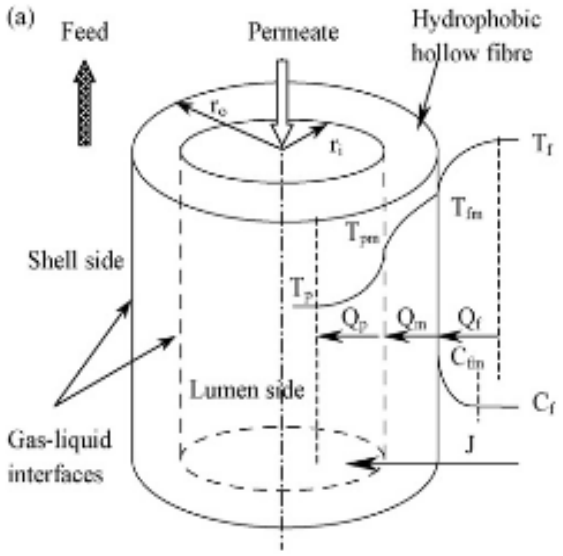

Figure 1.5 Heat and mass transfer in DCMD [70]

El-Bourawi et al and Khayet (2006, 2011) [51, 71] describe the heat transfers occur in DCMD as followed

- Through boundary layer of feed solution

$$Q_f = h_f (T_{bf} - T_{mf}) \quad (1.9)$$

- Through the membrane

$$Q_m = h_m (T_{mf} - T_{mp}) + J_w \Delta H_v \quad (1.10)$$

- Through boundary layer of permeate

$$Q_p = h_p (T_{mp} - T_{bp}) \quad (1.11)$$

Where h_f is the heat transfer coefficient boundary layer of feed solution, h_m is the heat transfer coefficient of the membrane, h_p is the heat transfer coefficient boundary layer of permeate, T_{fm} and T_{pm} are interface temperature of membrane in feed and permeate side. ΔH_v is the latent heat of vaporization, J_W is the permeate flux.

The heat transfer coefficient of whole membrane can be calculated by:

$$h_m = \frac{k_g \varepsilon + k_s (1-\varepsilon)}{\delta} \tag{1.12}$$

Where: ε is the membrane porosity, k_g is the thermal conductivity of the gas filling membrane pores, k_s is the thermal conductivity of membrane materials.

- Temperature polarization coefficient (TPC)

The fact of temperature polarization causes the temperatures at the membrane surface to differ from the bulk feed temperatures measured in the feed and in the distillate. This phenomenon is present even when the feed is water and causes an important loss in driving force for transport with regard to the imposed driving force and also mass flux. The temperature polarization coefficient can be calculated by:

$$TPC = \frac{T_{mf} - T_{mp}}{T_{bf} - T_{bp}} \tag{1.13}$$

Where T_{mf}, T_{mp} are the temperatures of feed and permeate on membrane surface, T_{bf} and T_{bp} are the bulk temperatures of feed and permeate.

The coefficient is therefore the ratio of the actual driving force to the overall driving force. Moreover, the temperature polarization can be regarded as a defect of the DCMD process, which should be minimized. Normally, the temperature polarization coefficient is 0.4-0.7 for an appropriate system design.

1.2.8 Mass transfer in DCMD

In MD process, the mass transport is typically described by assuming linear relationship between mass flux (J_w) and the water vapor pressure different through the membrane distillation coefficient (B_m) as expressed below [72]:

$$J_w = B_m(p_{mf} - p_{mp}) = B_m\left(\frac{dP}{dT}\right)_{T_m}\left(T_{mf} - T_{mp}\right) \quad (1.14)$$

Where p_{mf}, p_{mp} are the partial pressure of water at the feed and permeate sides by using Antoine equation at the temperatures T_{mf} and T_{mp} respectively, T_m is the mean temperature in the membrane pore and dp/dT can be evaluated from the clausius-Clapeyron equation, combined with Antoine equation, to calculate the vapor pressure:

$$\left(\frac{dP}{dT}\right)_{T_m} = \frac{\Delta H_{v,w}}{RT_m^2}\exp\left(23.238 - \frac{3841}{T_m - 45}\right) \quad (1.15)$$

Where R is gas constant, $\Delta H_{v,w}$ is the vaporization of water that can be evaluated using the following equation [46]:

$$\Delta H_{v,w} = 1.7535T + 2024.3 \quad (1.16)$$

Where T is the absolute temperature in K and $\Delta H_{v,w}$ is in kJ/kg.

- Concentration polarization coefficient (CPC)

The phenomenon of CPC causes the concentration at the membrane surface to differ from the bulk concentration in the feed side. While the concentration rises, the concentration polarization should be added to temperature polarization which reduces the imposed driving force and as well as the mass flux. The concentration polarization, CPC, can be calculated by [73, 75]:

$$CPC = \frac{C_{mf}}{C_{bf}} \quad (1.17)$$

Where C_{mf} and C_{bf} are indicate the membrane surface and bulk feed solution. The boundary layer concentration of non-volatile component C_{mf} can be expressed by:

$$C_{mf} = C_{bf} \exp\left(\frac{J}{\rho k}\right) \tag{1.18}$$

Where J is permeate flux ($kg/m^2.h$), ρ is the density of solute (kg/m^3), k is the mass transfer coefficient of solute.

In Eq. (1.18), the convective mass transfer coefficient, k, was estimated by applying the semi-empirical mass transfer model which was assumed to be analogous to the heat transfer model in the same domain. This assumption is generally accepted due to the similarity of the two transport process occurring in the same geometry. The analogous is defined in Table 1.5.

Table 1.5 analogous dimensionless numbers in heat and mass transfer

In heat transfer	**In mass transfer**
Nusselt numbers: $Nu = \frac{hd_h}{k}$	Sherwood numbers: $Sh = \frac{Kd_h}{D}$
Reynolds numbers: $\mathrm{Re} = \frac{v\rho d_h}{\mu}$	Reynolds numbers: $\mathrm{Re} = \frac{v\rho d_h}{\mu}$
Prandtl numbers: $\mathrm{Pr} = \frac{C_p \mu}{k}$	Schmidt numbers: $Sc = \frac{\mu}{\rho D}$

Generally, heat transfer coefficient of boundary layers is evaluated using empirically correlated for determination of Nusselt number (Nu), Reynolds number (Re), and Prandlt number (Pr) [76]. The heat transfer coefficient of both feed and permeate sides could be demonstrated due to the different number of Reynolds between laminar and turbulent flow conditions [77, 78].

$$Nu = \left(\mathrm{Re}.\mathrm{Pr}.\frac{d_h}{L} \right)^{0.33} \qquad \mathrm{Re}<2{,}100 \qquad (1.19)$$

$$Nu = 0.023.\mathrm{Re}^{0.8}.\mathrm{Pr}^{0.33} \qquad \mathrm{Re}>2{,}100 \qquad (1.20)$$

1.2.9 Membrane fouling

Fouling is the major operating problems of the membrane distillation process. Fouling result decrease permeability due to the removal suspended or dissolved on the membrane surface. Various types of fouling have been studied in membrane system such as biological fouling, scaling, colloidal fouling and organic fouling. Lawson et al,. (1997) [54] revealed that fouling in MD is less of a problem than other membrane separation. Gryta, (2008) [79] investigated the performance of fouling during the concentration wastewater with protein and brine solution by using DCMD. The morphology and structure of the fouling layer were studied using Fourier transform infrared with diffuse reflectance spectroscopy (FTIR) and scanning electron microscopy (SEM). It was found that the fouling was built not only on the membrane surface but also in the membrane pore. As a result in their occurrence, it was found the efficiency of MD could reduce fouling more than 50 percents. Alklaibi and Lior, (2005) [47] proposed that pre-treatment is very important to preserve the membrane fouling and in order to enhance the permeate flux.

1.3 Objectives

The main objectives of this research are:

- To design and set up the new experiment of direct contact membrane distillation (DCMD) process.
- To study the feasibility of direct contact membrane distillation for recovers some valuable compounds such as protein, sucrose and pure water product.
- To evaluate the effect of operating condition on direct contact membrane distillation performance.

1.4 Scope of work

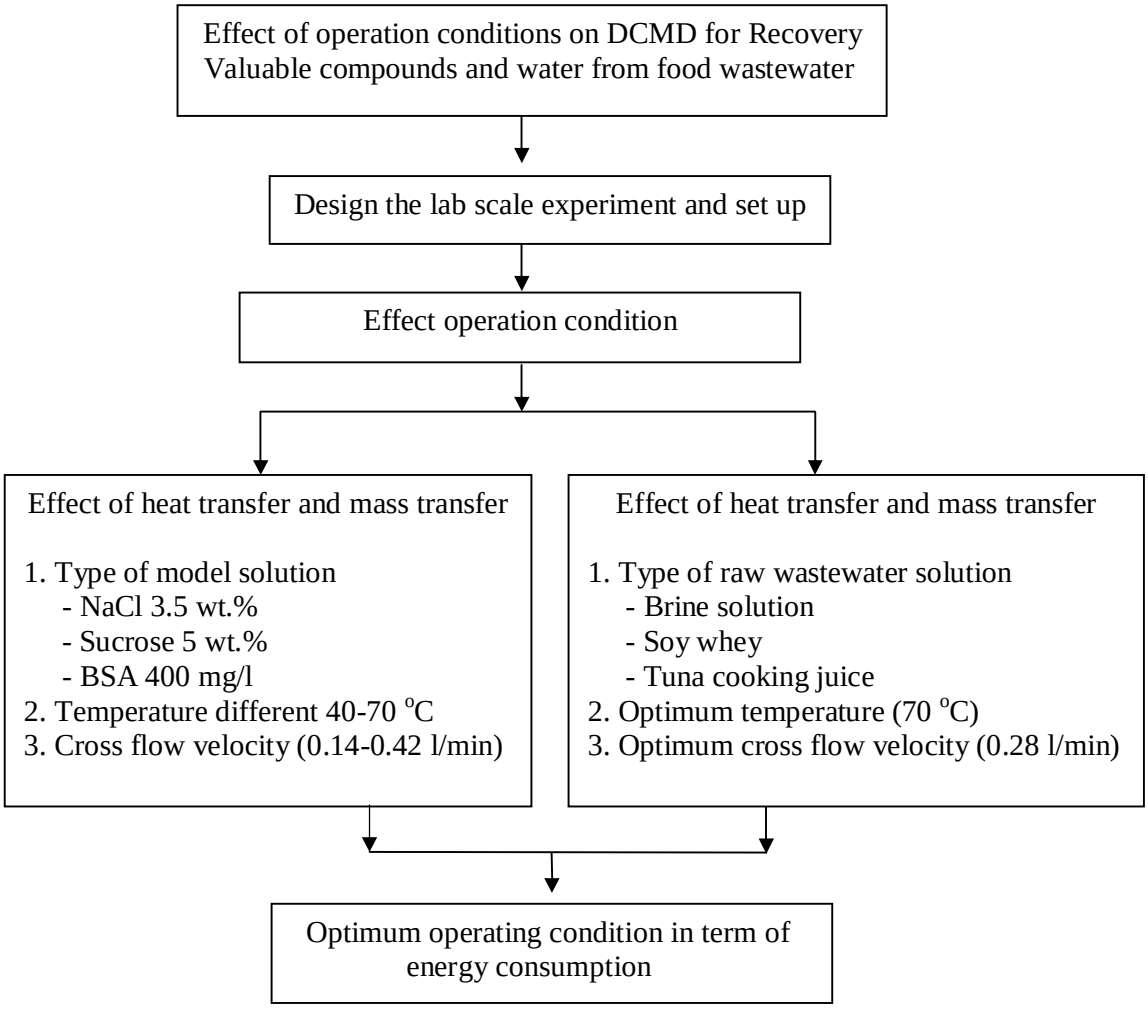

Figure 1.6 Flow chart of scope work

Chapter 2
Research Methodology

The experiments in this section are divided into three parts for recovery and concentrate of three wastes from desalination plants, Tofu whey household factory, and Tuna canning industry. The first part is the experiments performed with 3.5 % of NaCl solution (synthesis solution) and brine solution (real wastewater) for feed solutions. The second part was carried out with 5 % of sucrose solution (synthesis solution) and Tofu whey (real wastewater) for feed solutions, and the third part was applied with bovine serum albumin (BSA as synthesis solution) and tuna cooking juice (real wastewater) for feed solutions. All experiments were carried out at Membrane Science and Technology Research Center (MSTRC).

2.1 Materials

2.1.1 Preparation of synthesis solution

2.1.1.1 Sodium chloride (NaCl)

The sodium chloride (NaCl) was obtained from Sigma Aldric. A 3.5 wt. % of NaCl was prepared by mixing the NaCl and Ro water using a magnetic stirrer for 30 min at room temperature (30 ^{o}C). 5 L of 3.5 wt. % of NaCl solution was used as the feed solution for each experiment.

2.1.1.2 Sucrose

The sucrose was obtained from the commercial used. Before starting the experiment, sucrose was prepared the stock solution. A 5 Brix ($^{\circ}$B) of the sucrose stock solution was used as feed solution.

2.1.1.3 Bovine serum albumin (BSA)

The BSA powder (cold ethanol precipitated, 98-99%, A3350, Lot36H0417) was obtained from Sigma Chemical Co, St Louis, MO, USA. A 0.04 wt.% of BSA solution was prepared by mixing the BSA powder and RO water using a magnetic stirrer for 30 min at room temperature (30 ^{o}C). 5 L of BSA solution was used as feed solution for each experiment.

2.1.2 Preparation of brine solution

Brine solution was supplied by Cocacola Company Limited from Surat thani provine, Thailand. The brine solution was collected from reverse osmosis treatment discharged. The sample was stored at ambient temperature until required further experiment or analysis.

2.1.3 Preparation of tofu whey

Tofu whey was supplied from homemade process in Hat Yai district, Songkla province, Thailand. The hot tofu whey was collected and transfer to laboratory immediately. The suspended solid in tofu whey was removed by using cotton filtration. The sample was stored at 2-4 °C until required further experiment or analysis.

2.1.4 Preparation of tuna cooking juice

Tuna cooking juice was supplied by canned tuna processor, Tropical Canning (Thailand) Public Company Limited (Hat Yai). The suspended solid in tuna cooking juice was removed by cotton filtration. The pre-treated sample was heated at 60 °C, holding time of 10 min and kept overnight at 4 °C for fat removal and stored at -20 °C until required for further experiment or analysis [38].

2.1.5 Membrane

A hollow fiber PVDF (Polyvinyledene Fluoride) membrane was supplied from Econity, (South Korea)with normal pore size of 0.1 μm, porosity 70 %, membrane thickness 250 μm, and membrane length 240 mm. The overall characteristics are presented in Table 2.1.

Table 2.1 Characteristics of PVDF hollow fiber membrane

Parameters	**Value**
Hollow fiber membrane	Polyvinyledene Fluoride (PVDF)
Contact angle (°)	90.4
Porosity (%)	70
I.d of fiber (mm)	0.7
O.d of fiber (mm)	1.2
Mean pore size (μm)	0.1
Thickness (μm)	250
Effective length (mm)	240
Number of fiber	11
Effective area (m^2)	0.01

*I.d: Inner diameter membrane

O.d: Outer diameter membrane

The characteristics of the flow through the shell and lumen sides are listed in the Table 2.2.

Table 2.2 Membrane module characteristics and channel dimensions

Membrane module	Module outer diameter (m)	Module inner diameter (m)	Length (m)	Hydraulic diameter (m)	Effective membrane area (m^2)
Shell flow	1.5×10^{-2}	9×10^{-3}	2.4×10^{-1}	4.2×10^{-3}	5.91×10^{-5}
Lumen flow	1.5×10^{-2}	9×10^{-3}	2.4×10^{-1}	7×10^{-4}	4.23×10^{-6}

- Membrane module design

A cross flow PVDF hollow fiber membrane and cylinder module have been studied omit the heat transfer limit. The hollow fibers were arranged in staggered fashion in the cylinder module. The liquid was carried out to the shell side of cylinder module. Within the well-designed of the module, it allowed the hot feed solution to flow freely in cross flow outside and perpendicular to the fibers in the module. The material of this module was using clear acrylic cast plastic with a reasonable thickness and heat transfer resistance. The two ended bundles of the membrane were sealed with solidified epoxy resin to form a membrane module.

2.1.6 Instruments

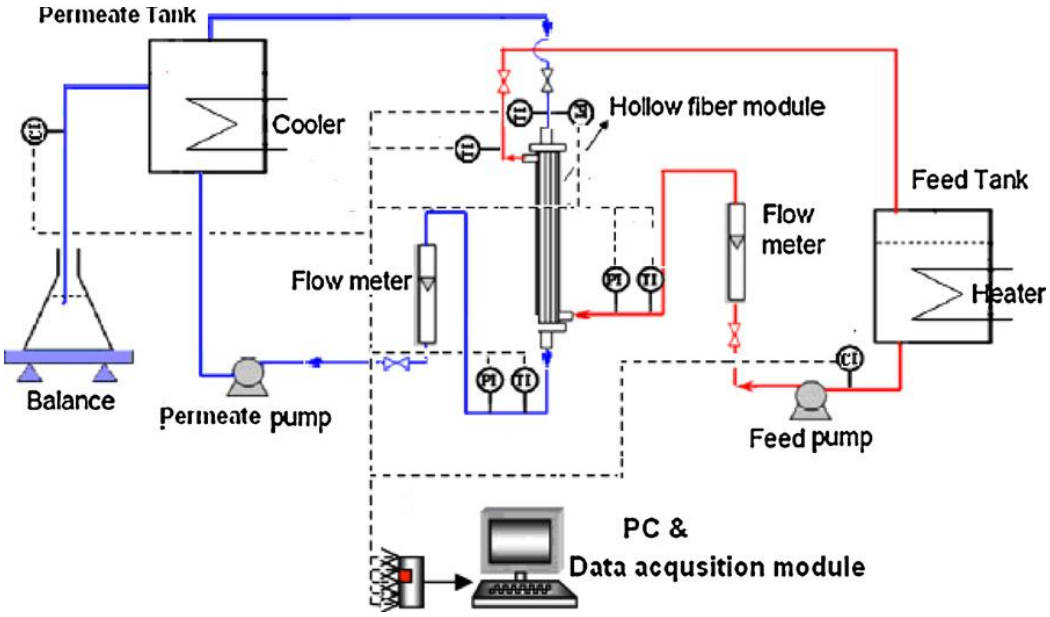

Figure 2.1 Experiment set up of DCMD diagram

The unit for DCMD experiments was designed and fabricated in our Membrane Research Laboratory. It divided into three parts: feed, membrane module, and permeate. The schema of DCMD process was illustrated in Figure 2.1 with the numbers indicating the following items.

2.2 Experimental procedure

2.2.1 Analytical method

The salt concentration (assessed by measuring conductivity) and pH were measured at regular intervals thought out each run. The samples of feed side of the synthesis solutions and real wastewater were collected 30 min interval each run and at the end of each run for permeate side [80]. The protein content was determined by using Lowry method [81-82]. The samples were diluted to ensure that the measured absorbance was <1.0. The viscosity was measured by capillary viscometer, the sucrose content was measured by using refractometer (°Brix) (see Appendix A). The conventional parameter for wastewater treatment such as COD, SS, Total nitrogen (TN), ammonia nitrogen (NH_3-N), Total phosphorous (TP) were determined according to AWWA (2012) methods [83].

The experiment setup was performed in circulation mode using hollow fiber membrane in DCMD. The membrane module was installed in vertically to omit the effect of free convection and air bubble removal. RO-deionized water was used as feed and permeate solutions. The feed solution was heated and maintained at the requirement temperatures by heater, and the permeate solution was maintained at the constant temperature by chiller. Both feed and permeate solutions were carried out into the shell side of the membrane module and flowed co-currently. The solutions were circulated through the close loop system.

2.2.2 Performance test

The performance test was carried out in close loop to the membrane module. The RO-deionized water was operated in both feed and permeate sides. The feed solution was heated and maintained to the required temperature by heater model ED JULABO with Temperature stability ±0.03 ℃ and carried out to the shell side of the membrane. The feed temperature was varied from 40 ℃ – 70 ℃. Simultaneously, the permeate solution water was cooled down to the constant temperature at 20 ℃ by chiller model HAILEA HS-66A. The temperature at inlets and outlets of both feed and permeate sides were measured by thermometer. The pressures were measured by pressure gauges which connect to data logger model Luthron MPS 384SD. On the other hand, permeate was fed into the lumen side of the membrane. Both feed and permeate were operated by peristaltic pump model Master flex and adjusted the cross flow rates. The feed and permeate temperature were recorded for interval time. The over water level of the permeate flux was recorded by using an analytical balance model AND, GF-3000 with accuracy ±0.01g.

The DCMD experiments of this study were performed with 3 different cross flow velocities for each temperature condition. The experimental conditions are listed in Table 2.3.

Table 2.3 Operating conditions of the experiment

Run	Temperature (°C)		Velocities (m/s)		Reynolds number (dimensionless)	
	Feed	Permeate	Feed	Permeate	Feed	Permeate
1	40	20	0.14	1.97	900	1,372
2	50	20			1,081	1,372
3	60	20			1,250	1,372
4	70	20			1,449	1,372
1	40	20	0.28	1.97	1,801	1,372
2	50	20			2,126	1,372
3	60	20			2,500	1,372
4	70	20			2,898	1,372
1	40	20	0.42	1.97	2,701	1,372
2	50	20			3,243	1,372
3	60	20			3,751	1,372
4	70	20			4,347	1,372

2.2.3 Synthesis solutions performance

The experiments were performed with different synthesis solutions to represent the real wastewater of Brine solution, Tofu whey, and Tuna cooking juice by using 3.5 wt.% of NaCl, 5 wt.% of sucrose, and 400 mg/l of BSA, respectively.

The synthesis solutions performance test was carried out in close loop to the membrane module. The feed solution was heated and maintained to the required temperature by heater and carried out to the shell side of the membrane. The feed temperature was using the varied from 40 °C – 70 °C. Simultaneously, the RO-

deionized water was used as permeate and cooled down to the constant temperature at 20 °C by chiller. The temperature at inlets and outlets of both feed and permeate sides were measured by thermometer. The pressures were measured by pressure transducers which connect to data logger. On the other hand, permeate was fed into the lumen side of the membrane. Both feed and permeate were operated by peristaltic pump and adjusted the cross flow rates. The feed and permeate temperature were recorded for interval time. The sample was collected for 30 min for interval time keep preserved in the refrigerator at 4 °C. The over water level of the permeate flux was recorded by using an analytical balance.

2.2.4 Real wastewater performance

The real wastewater performance was followed the application of the synthesis solution performance by using the optimum value which obtained from the synthesis solution. The feed and permeate temperature were recorded for interval time. The sample was collected for 30 min for interval time and analyzed after each run. The over water level of the permeate flux was recorded by using an analytical balance.

2.2.5 Cleaning mode

Membrane cleaning was taken place through the external and internal cleaning in CIP mode (clean in place). The membrane module was flushing with RO-deionized water for 30 min. Then, the membrane was rinsed with chemical reagent for 30 min and finally, the membrane module was re-rinsed with RO-deionized water until the neutral pH. The various chemical reagent used in this study are presented in Table 4. The cleaning efficiency was calculated as the ratio between flux before and after cleaning the membrane (J/J_o).

2.2.5.1 External cleaning mode

Membrane cleaning was carried out through the shell side with flow rate approximately 1000 ml/min at feed side and 500 ml/min at permeate side. The solution of feed side was flushed to the hollow fiber module to remove the deposit on membrane surface without pass through to the membrane pore. The system was operated in ambient temperature.

2.2.5.2 Internal cleaning mode

The internal cleaning was taken to account to consider the most effective cleaning mode. The reagents solution was applied to hollow fiber module in shell side of the membrane and on the permeate side; the RO-deionized water flew bottom-side up and directly to discharge likewise the microfiltration mode. The flow rate of both feed and permeate sides were carried out at 1000 ml/min and 500 ml/min and in ambient temperatures, respectively.

Table 2.4 Chemical cleaning agent and cleaning protocol used in the lab-scale cleaning

Types of feed solution	Cleaning reagent	References
NaCl 3.5 wt.% Brine solution	DI water, 2 wt.% of citric acid	[84]
Sucrose Tofu whey	2 wt.% of citric acid, a.5 wt.% of NaClO	[85]
BSA Tuna cooking juice	2 wt.% of citric acid, 2 wt.% of NaClO, 1.5 wt.% of HCl	[84, 85]

Chapter 3
Results and discussion

3.1 Characteristics of real wastewater

3.1.1 Brine solution

The chemical properties of brine solution are shown in Table 3.1. The results of solute rejection test are reached to 99.99 % at pH in range of 7.0 and 9.0, which indicated that the membrane had no leakage and no significant influence of fouling on the membrane surface during the DCMD process. All the results showed that the membrane was suitable for DCMD application in salt removal from the brine solution.

Table 3.1 Chemical compositions of brine solution at feed, concentrate, permeate side and percent rejection

Brine solution	Feed side	Concentrate	Permeate side	Percent rejection (%)
pH	8.22	8.97	7	-
Conductivity (mS/cm)	10.2	17.5	0.0004	99.99
TDS (mg/l)	6,530	11,200	0.25	99.99
Salinity (mg/l)	7,171	12,302	0.28	99.99

3.1.2 Tofu whey

The performance of DCMD system is presented in percent rejection and % recovery. For tofu whey recovery in water production obtain for 12.79 kg/m^2.h and the salt rejection is reach to 99.99 %. Moreover, 26.21 wt.% of sucrose was recovered from tofu whey. The wastewater characteristic of feed and permeate of tofu whey are shown in Table 3.2**.**

Table 3.2 Chemical compositions of tofu whey at feed, concentrate, permeate side and percent rejection

Compositions	Tofu whey feed	Tofu whey concentrate	Tofu whey permeate	Tofu whey rejection (%)
pH	6.45	6.55	6.5	-
TS (mg/l)	3,660	4,097	71	98.06
TKN (mg/l)	335	375	12	96.42
BOD (mg/l)	3,352	3,752	27	99.19
COD (mg/l)	9,445	10,572	141	98.51
Sucrose (mg/l)	11,000	13,000	ND	100
Protein (mg/l)	2,494	2,649	ND	100
PO_4-P (mg/l)	13	15	1.1	91.82
TOC (mg/l)	100	112	4.5	95.52
TDS (mg/l)	4,125	4,617	22	99.47
Ash (%. w/v)	0.14	0.16	0.002	98.57
Salt concentration (mg/l)	4,460	4,992	0.7	99.98
Conductivity (mS/cm)	6.47	6.21	0.001	99.98
Turbidity (NTU)	104	116	ND	100

*ND: Not Detected

3.1.3 Tuna cooking juice

Percent recovery of real waste water was achieved during DCMD as represent in Table 3.3.

Table 3.3 Chemical compositions of tuna cooking juice at feed, concentrate, permeate side and percent rejection

Compositions	Tuna cooking juice feed	Tuna cooking juice concentrate	Tuna cooking juice permeate	Tuna cooking juice rejection (%)
pH	6.33	6.45	6.6	-
TS (mg/l)	11,450	12,237	17	99.85
TKN(mg/l)	620	663	ND	100
COD(mg/l)	19,033	20,341	<5	99.97
Protein (mg/l)	9,200	11,408	ND	100
TDS(mg/l)	12,510	133,369	25.5	99.79
Salt concentration (mg/l)	11,476	12,654	0.026	99.99
Conductivity (mS/cm)	15.5	18	0.0012	99.99
Turbidity (NTU)	715	764	ND	100

*ND: Not Detection

In comparison, approximately 17 % to 50% water flux recovery of brine solution was higher than tofu whey and tuna cooking juice. As the results it was expected that the flux recovery would be higher due to the pre-treatment and cross flow velocity take place. On the other hand, 32.53 wt. % were obtained from recover tuna cooking juice, respectively.

3.2 Performance of the system

3.2.1 Effect of temperature on permeate flux

The experiments were carried out with various synthesis and real wastewater solution at a range of temperatures, 40, 50, 60, and 70 °C, respectively. The highest permeate flux was obtained at the feed temperature of 70 °C. Generally the feed temperature was the driving force to increase vapor pressure of the DCMD system [86]. When the feed temperature increases, it leads to improve the heat transfer coefficient (h_f) and induce to higher sensible heat loss which supports the increased permeate flux. As shows in Figure 3.1, 3.2 and 3.3, the variation of permeate flux increased with increasing the feed temperature. It can be seen that the feed synthesis solution of NaCl and sucrose were obtained similar flux at the feed temperature of 70 °C, otherwise at the low feed temperature in range of 40 to 60 °C was a little different. Generally, as the feed temperature increases the structure of BSA molecule on membrane surface undertaken conformational changes in form of unfolding, which reduces the electrostatic repulsion between BSA molecule and between BSA and membrane surface. This can cause the viscosity of sucrose at low temperature to be higher than that at the high temperature. Furthermore, unfolding of BSA at high temperature leads to increase the hydrophobic interactions between BSA molecules causing to higher rate of deposit [87]. These results can be concluded that the temperature increasing, the permeat flux reaches 0.34 $kg/m^2.h$ for sugar and NaCl while the BSA increased in exponential function. On the other hand, it can be observed that the permeate flux curve of BSA was the lowest amount in the synthesis solution. Then, the systems obtain higher flux at high temperature than that at low temperature but the rate of increasing and the functional depend on types of solution.

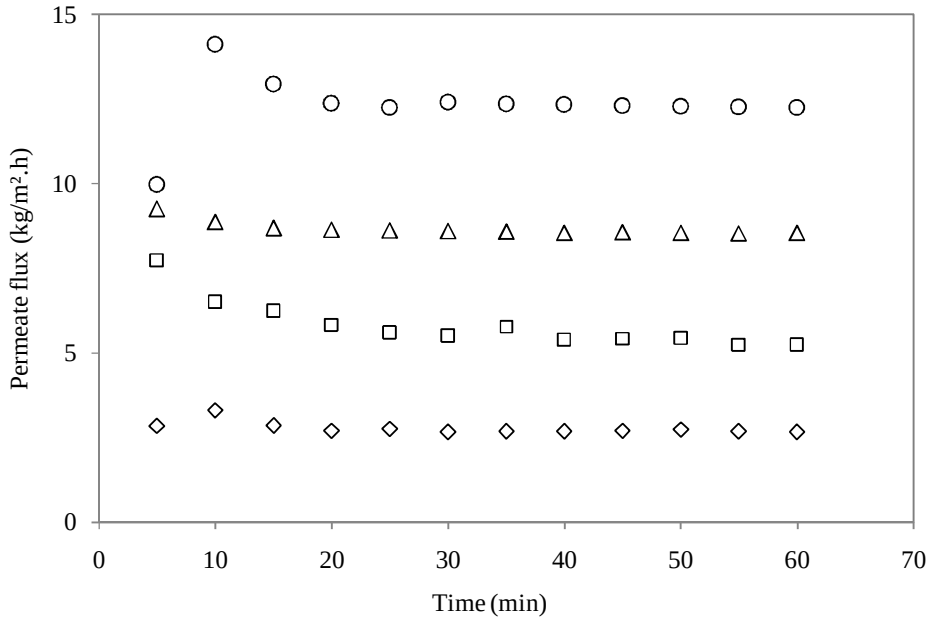

Figure 3.1 Permeate flux versus operating time during MD of 3.5 wt.% NaCl at 0.28 m/s as varying by temperature (○) 70 °C; (Δ) 60 °C; (□) 50 °C; (◊) 40 °C

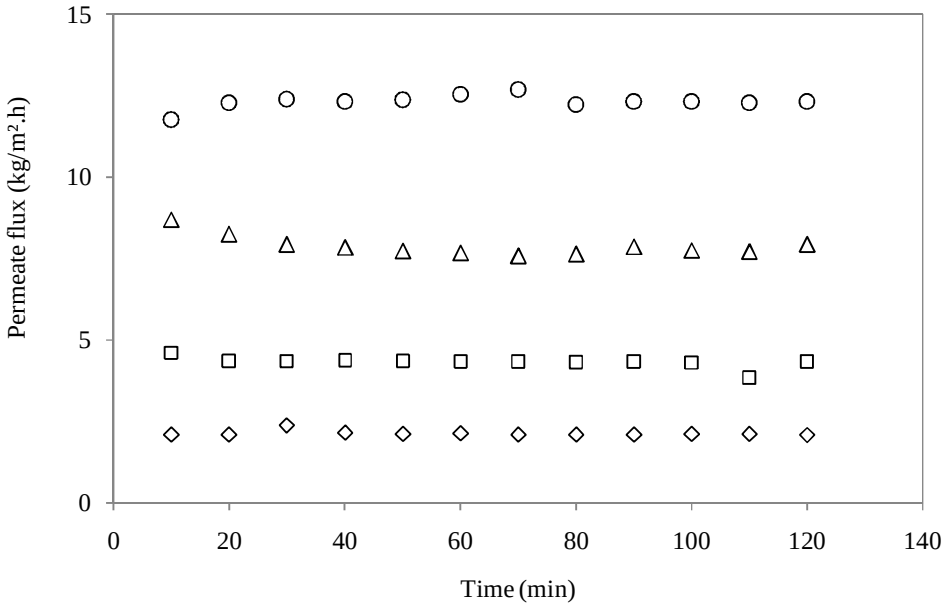

Figure 3.2 Permeate flux versus operating time during MD of 5 wt.% sucrose at 0.28 m/s as varying by temperature (○) 70 °C; (Δ) 60 °C; (□) 50 °C; (◊) 40 °C

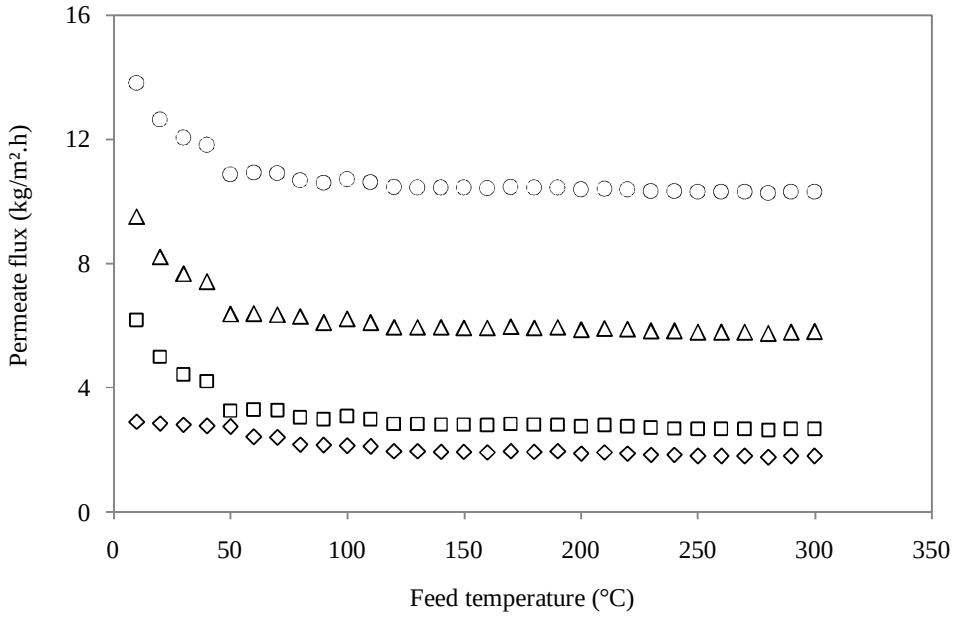

Figure 3.3 Permeate flux versus operating time during MD of 0.04 wt.% of BSA at 0.28 m/s as varying by temperature (○) 70 °C; (Δ) 60 °C; (□) 50 °C; (◊) 40 °C

3.2.2 Effect of cross flow velocity on permeate flux

The DCMD experiments were performed by using PVDF hollow fiber membrane to investigate effect of velocity on permeate flux. A results of the different solutions and as well as each velocities are presented in Figure 3.4, 3.5, and 3.6. These experiments were carried out with feed and permeate temperature of 70 °C and 20 °C (ΔT=50°C), respectively. Results indicate that permeate flux increases with increasing flow velocity. This was expected due to enhanced mixing in the flow channel and a decrease in the thickness of the temperature boundary [88-90]. At high flow rates, high turbulence will increase the heat transfer so as to increase the interface temperature and permeate flux, but the high turbulence will also incur a higher compressive pressure on the membrane surface. The real wastewater obtained lower flux values than synthesis solution. This is most likely due to the thicker of substance imposed higher of resistance to vapor diffusion on pores size of the membrane and results in lower permeate flux [54, 88].

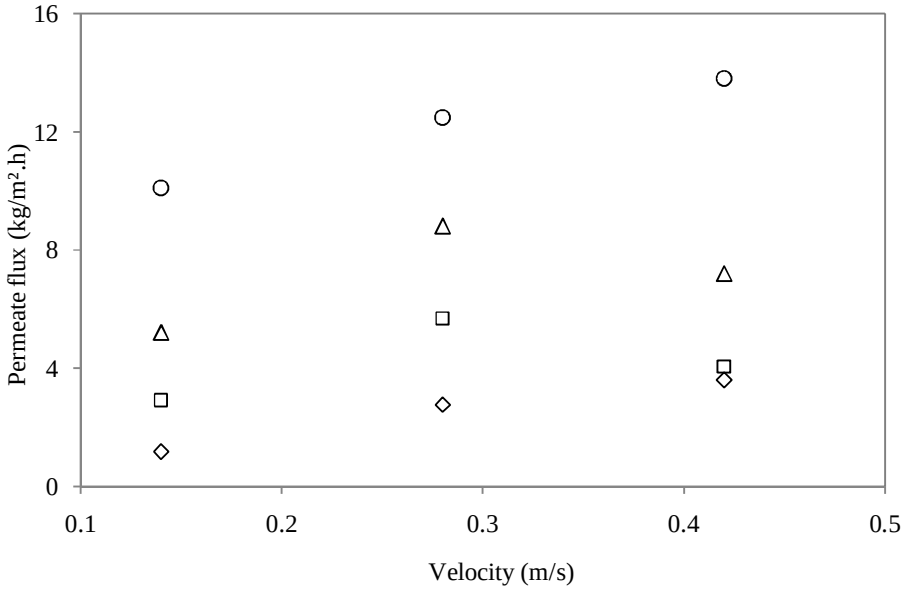

Figure 3.4 Permeate flux versus cross flow velocity of 3.5 wt.% of NaCl at feed temperatures (○) 70 °C; (Δ) 60 °C; (□) 50 °C; (◊) 40 °C

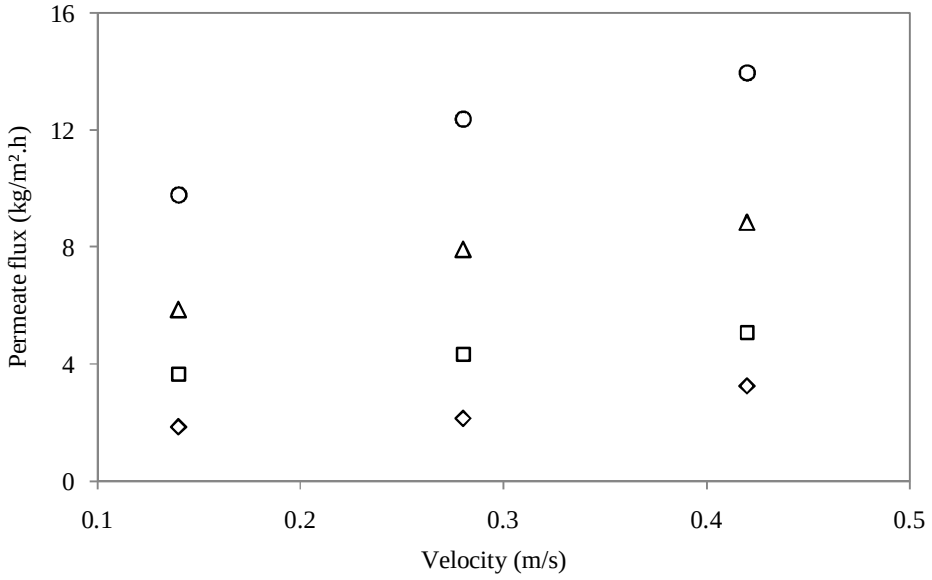

Figure 3.5 Permeate flux versus cross flow velocity of 5 wt.% of sucrose at feed temperatures (○) 70 °C; (Δ) 60 °C; (□) 50 °C; (◊) 40 °C

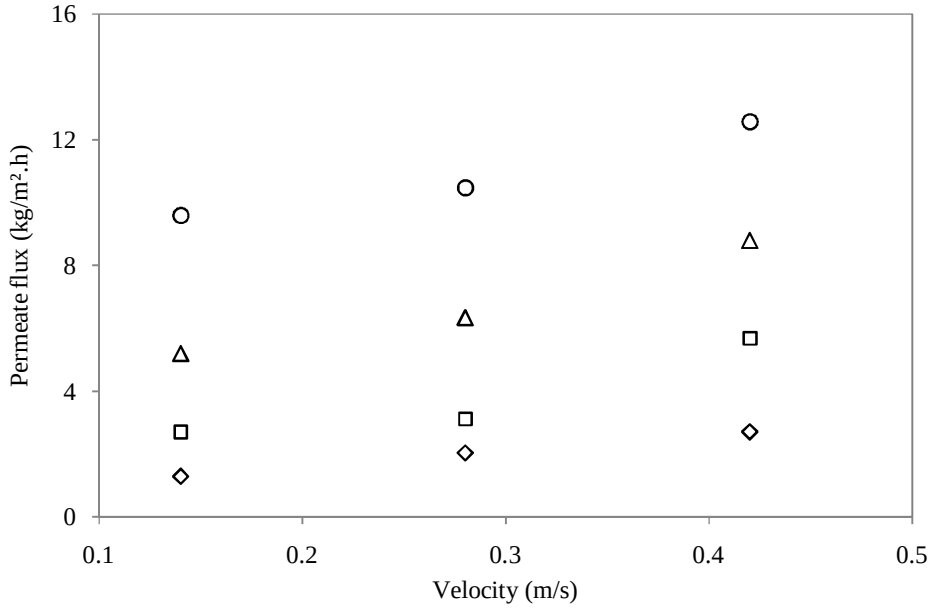

Figure 3.6 Permeate flux versus cross flow velocity of 0.04 wt.% of BSA at feed temperatures (○) 70 °C; (Δ) 60 °C; (□) 50 °C; (◊) 40 °C.

3.2.3 Effect of feed solution on permeate flux

The obtained results confirmed a significant influence of the different feed solution on the process efficiency of permeate flux. The experiments were performed with three synthesis solution before applied the real wastewater. It can be seen in Figure 3.7 that the permeate flux of NaCl and brine solution were obtained similar level about 12.79 kg/m².h. On the other hand, the permeate flux of sucrose and tofu whey was obtained in range of 12.38 kg/m².h and 10.59 kg/m².h. Due to tofu whey contains the organic compounds that undergo transformation into the membrane surface, which causes the reduction of permeate flux.

Apparently, the tuna cooking juice permeate flux decline became much faster than BSA since tuna cooking juice contain substance of high salt concentration, proteins and other various compounds. The interaction of hydrophobic between proteins molecule and hydrophobic membrane was represented the ability of fouling being sucked [91, 92].

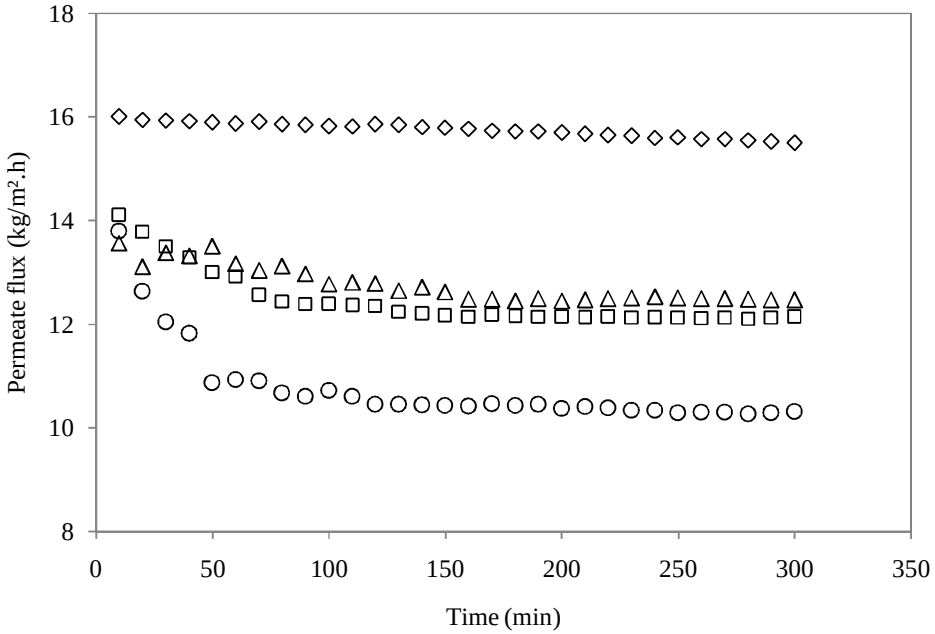

Figure 3.7 Permeate flux versus operating time of different feed solutions (◊) DI water; (Δ) 5 wt.% of Sucrose; (□) 3.5 wt.% of NaCl; (○) 0.04 wt.% of BSA at cross flow velocity of 0.28 m/s

3.2.4 Permeate flux of real wastewater

Theoretically, the feed concentration should have influence on the permeate flux. This study found that the difference of concentration between the synthesis and real wastewater flux variation incurred by the feed concentration about 33.26, 20.57, and <100 % for brine, tofu whey and tuna cooking juice, respectively. In terms of permeate flux decline pattern, a similar trend were observed for each synthesis and real wastewater in Figure 3.7 and 3.8. The 3.5 wt.% of NaCl showed a approach permeate flux declining pattern about 12.48 kg/m^2.h and 12.80 kg/m^2.h properly. Also, higher permeate flux decline was observed with 5 wt.% of sucrose, in comparison to the permeate flux of tofu whey. Consequently, 14.53% of permeate flux of tofu whey was less than 5 wt.% of sucrose about 12.39 kg/m^2.h to 10.59 kg/m^2.h. Beside, a faster permeate flux decline was discovered with tuna cooking juice compared to 0.04 wt.% of BSA. As a result, 46.37% of permeate flux of tuna cooking juice was slighter than BSA within about 10.48 kg/m^2.h to 5.62 kg/m^2.h.

Similar to other study results shown by Zhang et al, (2011) [93] conclude that the higher the concentration of the NaCl solution and protein are, the higher the results boiling point. The decrease in vapor pressure and less vaporization at the membrane surface causes a decrease in the amount of vapor flow through the membrane [94].

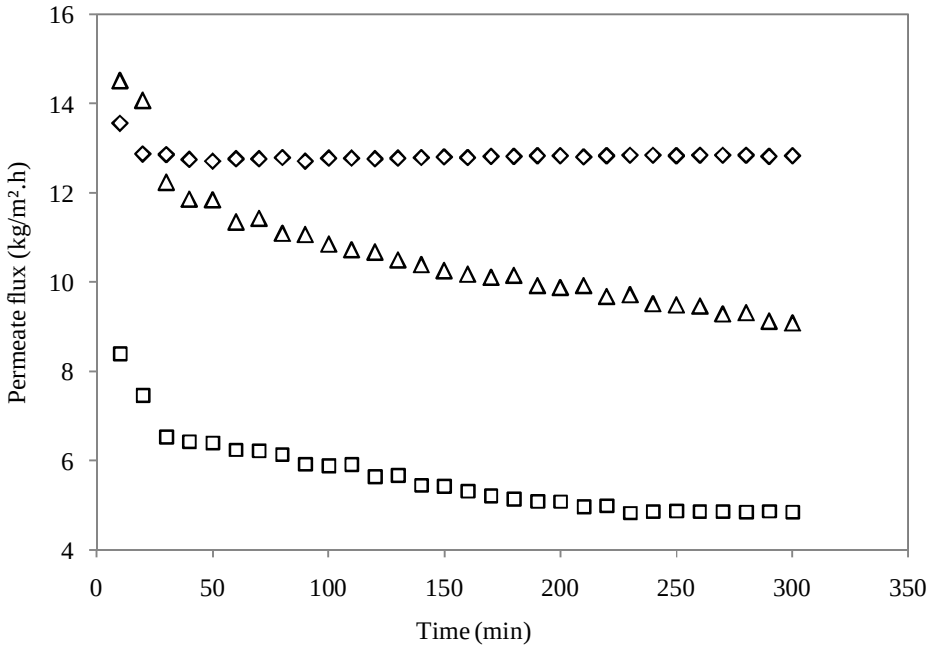

Figure 3.8 Permeate flux versus operating time of different feed solutions (◊) brine solution; (Δ) tofu whey; (□) tuna cooking juice at cross flow velocity of 0.28 m/s.

3.3 Effect of mass transfer on heat transfer rate and heat transfer analysis in DCMD

Mass flux for laminar and turbulent flow conditions were determined at each operating condition listed in Table 2.3. The measured fluxes were used to study the effects of mass transfer on heat transfer rates and heat transfer coefficients. In addition, it were applied to determine the significance function of each heat transfer mechanism, illustrated the temperature distribution inside the membrane, and to calculate the temperature polarization coefficients.

3.3.1 Temperature polarization coefficient

The effect of mass transfer on heat transfer coefficients were calculated by Eq. (1.9)-(1.12). The correlation significance of each heat transfer coefficient mechanism in feed, membrane, and permeate streams were analyzed by heat transfer coefficient model in Table 1.5.

The correlation of heat transfer coefficient between Nu_l (Nusselt number for laminar flow) and Nu_T (Nusselt number for turbulent flow) in this study were applied to propose the heat transfer correlation expressed as [73],

$$Nu = 1.86\left(\frac{Re.Pr.d_h}{L}\right)^{0.33} \qquad Re<2100 \qquad (3.1)$$

$$Nu = 0.023Re^{0.8}Re^{0.33} \qquad Re>2100 \qquad (3.2)$$

Figure 3.9, 3.10, and 3.11 show the temperature polarization coefficients (τ) in function of feed temperature of each synthesis solution (3.5 wt.% of sodium chloride, 5 wt.% of sucrose and 0.04 wt.% of BSA). According to the curves can be explained that the temperature polarization coefficients at feed velocity of 0.14 m/s were lower than 0.28 m/s and 0.42 m/s. Moreover, it decreased with increasing feed temperature due to higher energy consumption from vaporization at the feed to membrane surface at higher feed temperatures.

The temperature polarization coefficient can be determined by Eq. (1.13) which describes the effective temperature gradient across the membrane. The collaboration of heat transfer from the feed side over conduction and latent heat of vaporization with the vapor transport cause a decrease in temperature on the membrane surface and increase the corresponding the permeate temperature. As the result, the driving force between two phases reduces. Additionally, an increase in feed velocity improves the Reynolds number of the fluid and decreases the thickness of boundary layer. Consequently, the difference between temperature of bulk feed solution and membrane surface are decrease. As illustrated in Figure 3.12, the

increases in TPC with Reynolds number is quite significant at low values of Re. In transition region, the TPC values increases but the slope of the curve for this region is slightly decreases than that for the laminar. Moreover, the slope further decreases as the turbulent region is approached.

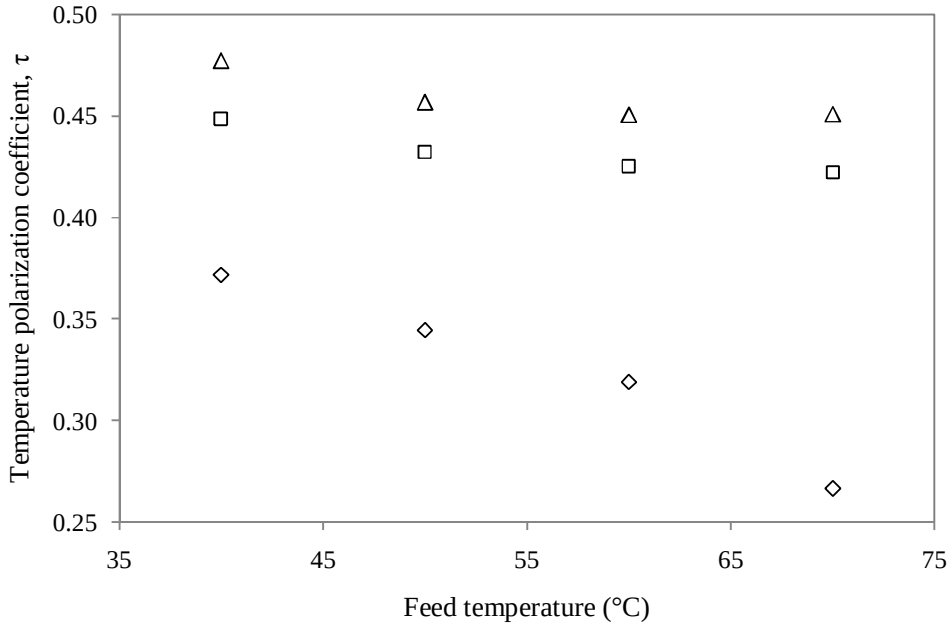

Figure 3.9 Temperature polarization coefficient at various feed temperatures for 3.5 wt.% of NaCl; (Δ) 0.14 m/s, (□) 0.28 m/s, and (◊) 0.42 m/s.

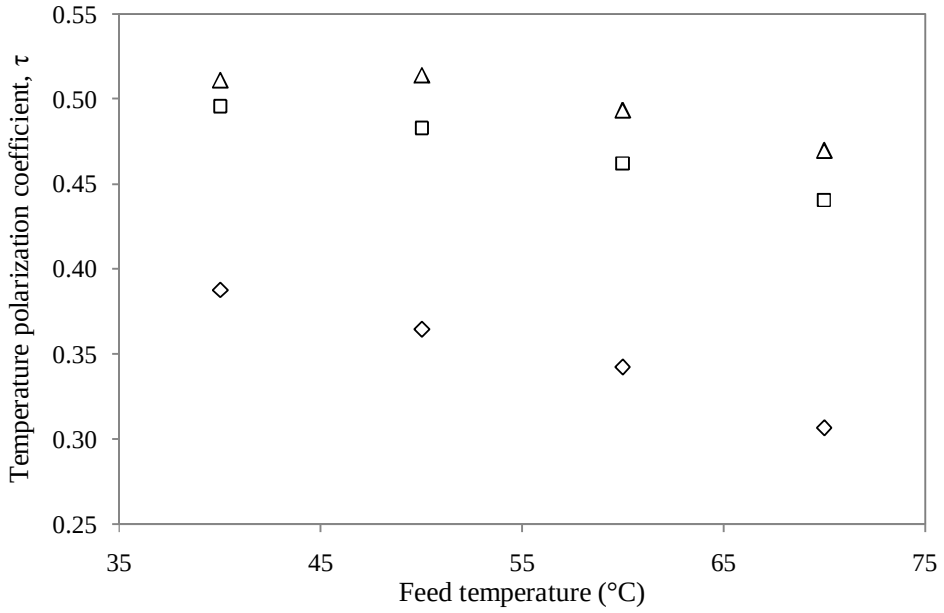

Figure 3.10 Temperature polarization coefficient at various feed temperatures for 5 wt.% of sucrose; (Δ) 0.14 m/s, (□) 0.28 m/s, and (◊) 0.42 m/s.

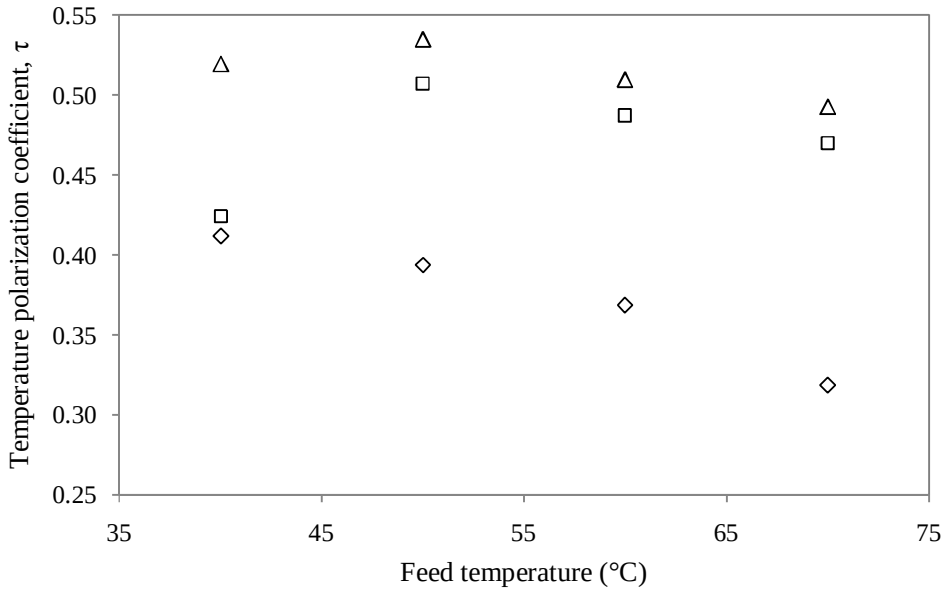

Figure 3.11 Temperature polarization coefficient at various feed temperatures for 0.04 wt.% of BSA; (Δ) 0.14 m/s, (□) 0.28 m/s, and (◊) 0.42 m/s

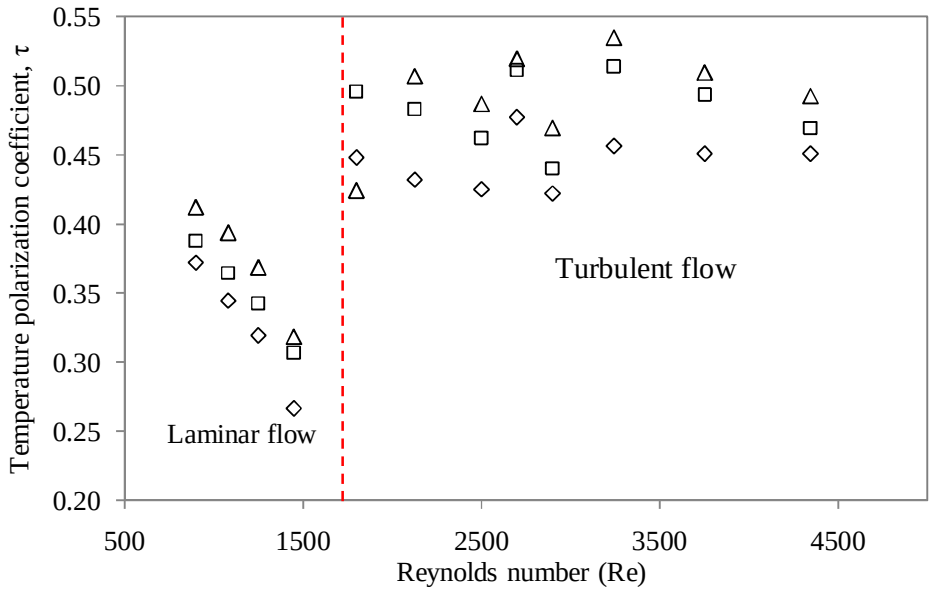

Figure 3.12 Temperature polarization coefficient at various feed temperatures for (◊) 3.5 wt.% NaCl, (□) 5 wt.% Sucrose, and (Δ) 0.04 wt.% BSA.

3.3.2 Concentration polarization coefficient

Typically, high mass transfer coefficient was found in pressure driven-based process. For instance, ultrafilration process (UF), nanofiltration process (NF), reverse osmosis (RO) and almost conventional processes which applied at high operating pressure. The effect of high mass transfer coefficient in UF process can be calculated from using Sherwood correlation for different flow mode. In this case study, the correlations of Sherwood for laminar Eq. (3.3) and turbulent flow Eq. (3.4) were summarized in Table 3.4.

Table 3.4 Mass transfer correlation in DCMD

Type	Correlation	Equation	Reference
Laminar flow	$Sh = 0.13Re^{0.64}Sc^{0.33}$	(3.3)	[73]
Turbulent flow	$Sh = 0.0233Re^{0.8}Sc^{0.33}$	(3.4)	[73]

Figure 3.13 shows the concentration polarization coefficient (CPC) versus the feed temperature difference at feed velocity of 0.28 m/s. As illustrated, the CPC were increased with increasing feed temperature. This is due to increasing in flux, which according to Eq. (1.17) and (1.18) the higher accumulation of feed concentration on membrane surface, consequently the concentration polarization is occurred [49]. The results can be illustrated that there were less concentration polarization occurred in feed boundary layer of NaCl and sucrose when the feed concentration were low and less significant effect on permeate flux. On the other hand, the concentration polarization of BSA was linear increased which leading to decrease permeate flux.

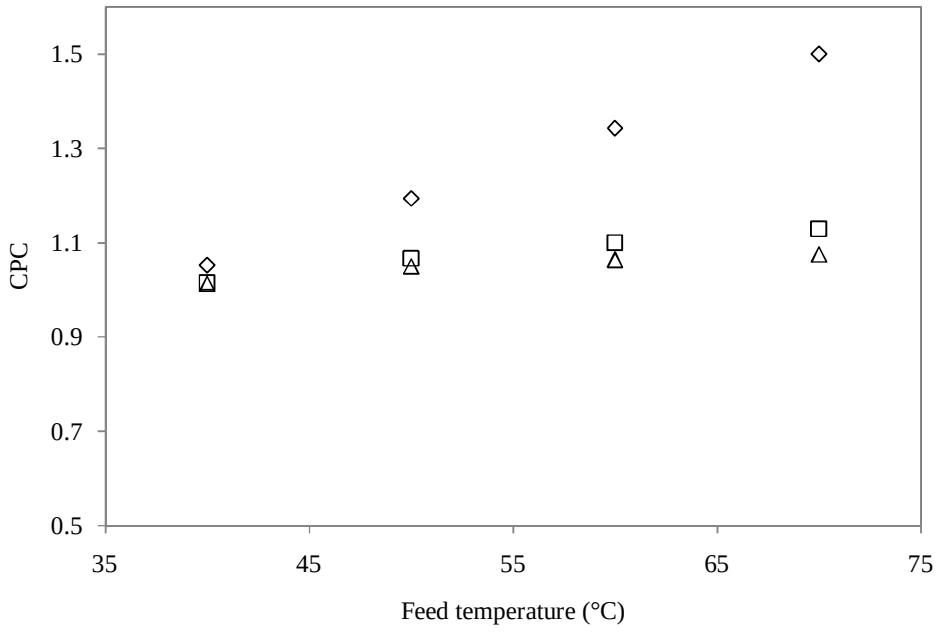

Figure 3.13 Concentration polarization coefficient at various feed temperatures for (◊) 0.04 wt.% of BSA; (□) 5 wt.% sucrose, and (Δ) 3.5 wt.% NaCl at feed velocity of 0.28 m/s

3.4 Fouling behavior

Generally, fouling is the aggregation deposits on the membrane surface or inside the pores of the membrane that degenerate the permeate flux and salt rejection performances [95, 96]. Fouling is one the major problems in membrane-based processes which could be a very harmful influence to the desalination and purification process. Generally, the foulants are colloidal in nature that interact with each other, or interact with membrane surface to form deposits.

3.4.1 Fouling behavior during the experiment

A feasible mechanism behind these fouling of tofu whey was investigated. As given in Figure 3.14 shows the flux versus long operating time in DCMD process for the membrane during fouling and after cleaning in different mode of synthesis solution of sucrose and real wastewater of tofu whey. The cleaning results of sucrose fouling presented over 100 % flux restoration after water flushing and acid cleaning. This result proves that the fouling of sucrose can be removed during cleaning process. However, the tofu whey was obtained over 100 % flux restoration at the starting time and the flux declined dramatically thereafter. It is proposed that the fouling is occurred by interaction of the various components which were consisted in solution such as sucrose (polysaccharide), proteins, and as well as sodium chloride in result leading to a marked flux decline. This could be due to whey components blocking the pores of the membrane [97]. In addition, sodium chloride is known as foulant, not only due to the precipitation, but also because it can affect the electrical layer of proteins much more and letting them to approach more closely. It can also act as a connector between the membrane and proteins, as well as between proteins [98, 99].

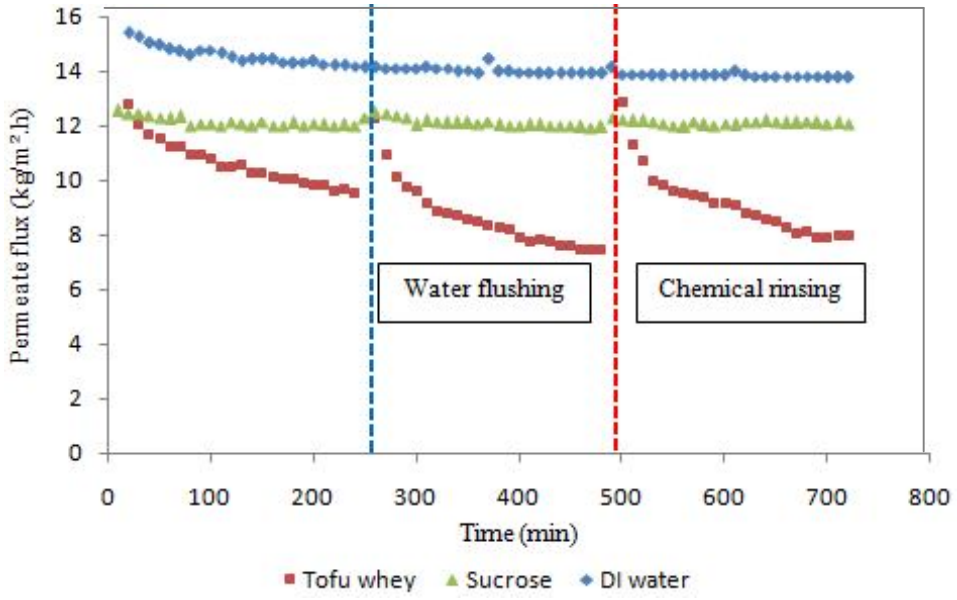

Figure 3.14 The dependence of permeate flux as a function of cleaning mode and working time of MD process. Feed: food wastewater containing NaCl, proteins and sucrose. Series: (□) Tofu whey, (Δ) Sucrose, and (◊) DI water. Feed flow 0.28 m/s at feed temperature 70 °C.

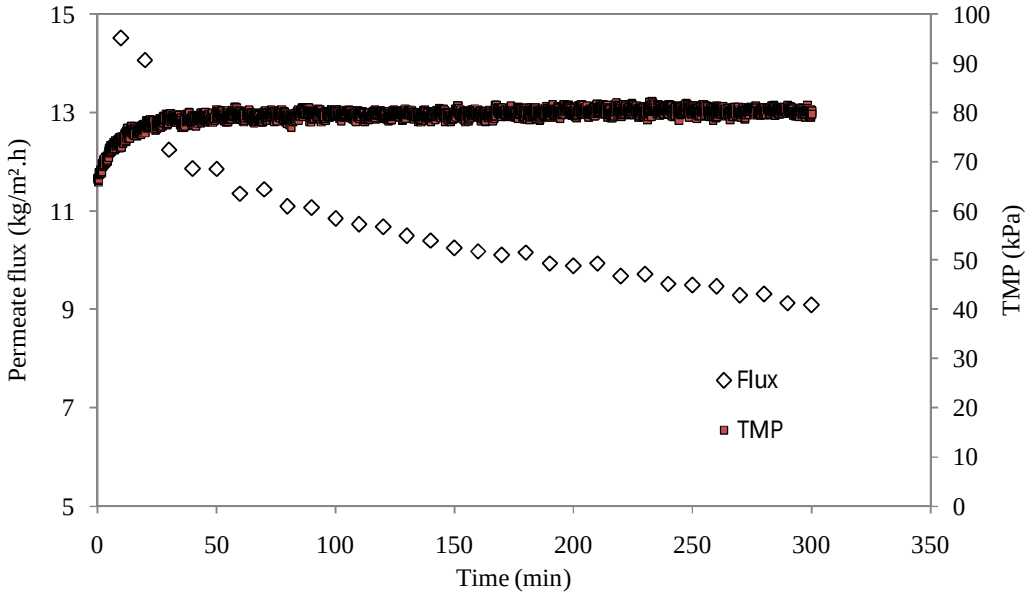

Figure 3.15 Permeate flux and transmembrane pressure versus operating time of tofu whey at feed velocity of 0.28 m/s with feed temperature of 70 °C and permeate temperature of 20 °C.

Figure 3.15 shows the permeate flux and transmembrane pressure versus operating time of tofu whey at feed velocity 0.28 m/s at feed temperature of 70 °C. The average of permeate flux about 10.59 kg/m².h was found at average TMP 79.41 kPa. It can be noticed that the permeate flux was decreased with increasing the TMP from 66.8 kPa to 79.7 kPa. Normally, high pressure supply could be eliminated the driving force which was the main point to generate the thermal efficiency since MD is the thermal-based process. In result leading to flux decline and the concentrated were also more serve at high TMP.

3.4.2 Morphology of membrane (SEM)

Fouling was found to be a large problem during concentrated water production from industrial wastewater by DCMD process. Gryta, (2008) [79] have been investigated fouling during concentrated saline wastewater from meat processing which consists sodium chloride, proteins and polysaccharide. The author revealed that the permeate flux was declined rapidly during DCMD process due to the deposits formed on membrane surface, which diminished the membrane permeability and increased temperature polarization.

After the completion of all experiment, the hollow fiber membrane was removed from the module to observe the fouling. Two points at the middle and the end of the fiber were selected for SEM test. Figure 3.16 shows the different affecting of membrane fouling: (a) shows the original membrane; (b) shows the deposit completely covered the membrane surface compared to the original membrane. Moreover, there were some particles which could be stuck on the membrane between the fibers and the seal resin of the module. And (c) shows the fouling membrane at the middle point of the fiber. At this point, it can be seen that the membrane surface also formed by the deposits like the previous point as well. The results show the effect of hydrodynamics to prevent the foulants on membrane surface.

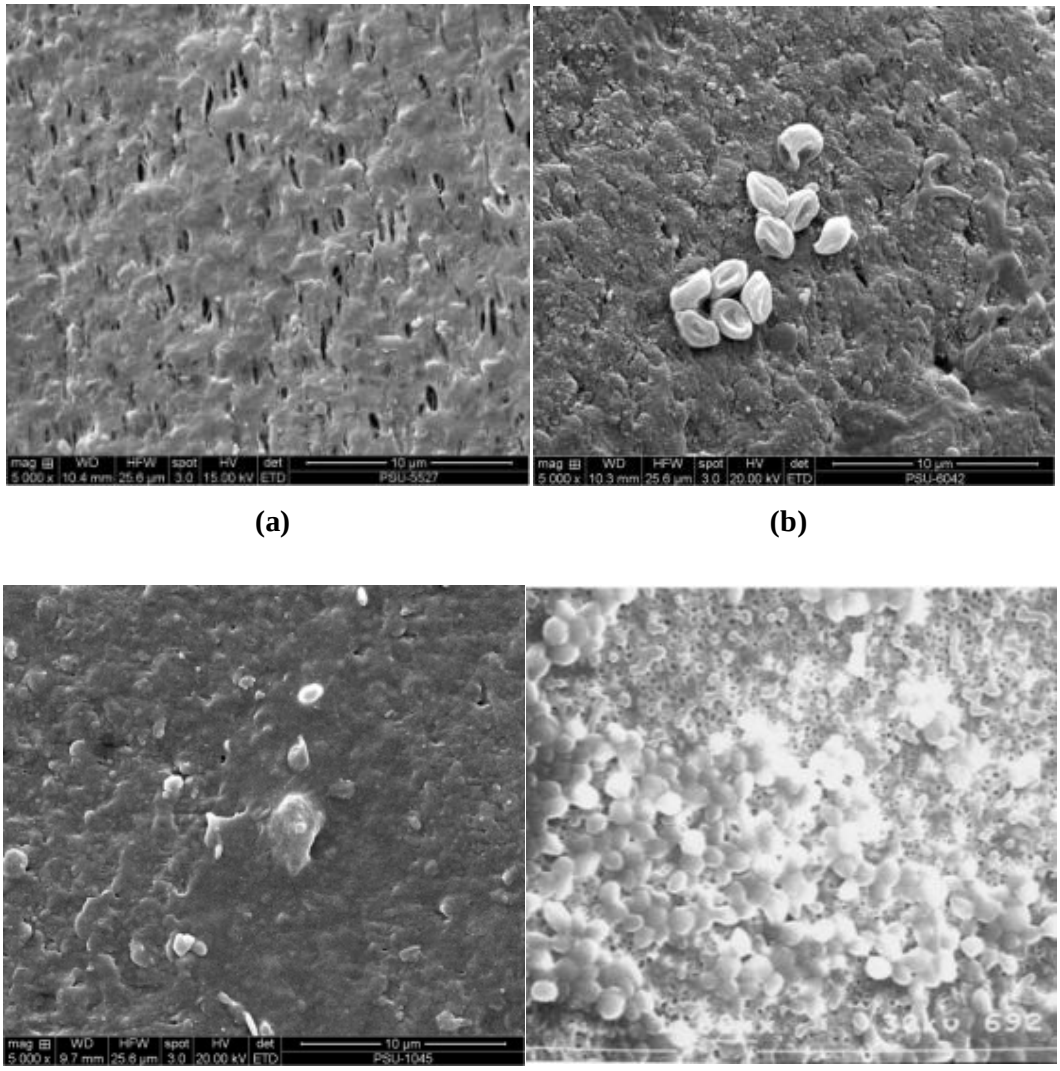

(a) **(b)**

(c) **(d)**

Figure 3.16 SEM pictures of the PVDF membrane: (a) original membrane, (b) fouling membrane at the top point, (c) fouling membrane at the middle point of the fiber, and (d) BSA fouled membrane, review [100].

Gryta, 2008 [79] reported that higher velocity would affect the growth rate of the fouling layer as well as the morphology and size of deposits and also porous deposits layer, while the lower velocity produced the thick deposits layer that found in this study as well.

However, in this study shows that the scaling was the major fouled on the membrane surface of the different solution either tofu whey or tuna cooking juice.

Kuberkar et al, 2001 [100] have studied the performance with and without crossflushing or backflushing by using yeast and BSA. Figure 3.16 (d) indicates SEM photograph of representative areas of the fouled membrane. The membrane surface was completely covered by cake in multilayer during the experiments. In this study could be concluded that the backflushing was only partially effective for removal of internal foulants during BSA experiments.

3.5 Energy consumption

The energy consumption of this process was assuming from the pump power needed for flow through the MD channel of both hot and cool side.

The equation used for obtained the heating and cooling energy is reported below:

$$Q_h = V_f \, Cp_f \, (T_{f,in} - T_{f,out}) \tag{3.5}$$

$$Q_c = V_p Cp_p \, (T_{p,in} - T_{p,out}) \tag{3.6}$$

When the Q_h and $Q_c$are the heating and cooling energy (W), V_f is the feed flow rate (kg/h), V_p is the permeate flow rate (kg/h), Cp_f is the feed specific heat (J/kg.K), Cp_p is the permeate specific heat (J/kg.K), $T_{f,in}$ and $T_{p,in}$ are the feed and permeate inlet temperatures (K), and $T_{f,out}$ and $T_{p,out}$ are the feed and permeate outlet temperature (K). The Table 3.5 shows the comparison in terms of permeate flux, energy consumption and evaporation efficiency among the different test.

Table 3.5 Energy consumption and evaporation efficiency of synthesis and real wastewater at permeate velocity of 1.97 m/s and T_f=70 °C and T_p=20 °C.

Solutions	V_f (m/s)	Energy consumption (W)	EE (%)	J (kg/m².h)
NaCl	0.14	283.05	37.75	10.11
	0.28	188.60	34.74	12.48
	0.42	240.36	36.65	13.80
Sucrose	0.14	230.53	35.80	9.80
	0.28	366.28	35.49	12.39
	0.42	377.68	36.69	13.96
BSA	0.14	298.10	29.34	9.60
	0.28	347.50	30.95	10.48
	0.42	533.02	34.43	12.14
Brine solution	0.28	369.83	37.19	12.80
Tofu whey	0.28	465.22	30.39	10.59
Tuna cooking juice	0.28	461.57	19.34	5.62

Table 3.5 was illustrated the comparison of energy consumption and evaporation efficiency in different feed solution of synthesis and real wastewater. The optimized results in terms of energy consumption and evaporation efficiency of synthesis solution was obtained at feed velocity of 0.28 m/s and temperature at 70 °C before applied with real wastewater. In terms of permeate flux, energy consumption and evaporation efficiency among the different of wastewater at optimized condition, it can be noticed that the permeate flux obtained were 12.48 kg/m².h, 12.39 kg/m².h, 10.48 kg/m².h for 3.5 wt.% of NaCl, 5 wt.% of sucrose and 0.04 wt.% of BSA which corresponding to the appropriate values of energy consumption were 188.60 W, 366.28 W, and 347.50 W, respectively. On the other hand, for the real wastewater which consists several of waste components also obtained the best result for each solution. As follows, the permeate flux about 12.80 kg/m².h, 10.59 kg/m².h and 5.62 kg/m².h were obtained from brine solution, tofu whey and tuna cooking juice, respectively. Even though the three real wastewater were obtained less permeate flux compared to synthesis solution, but the higher energy consumption were able to

supply to each wastewater about 369.83 W, 465.22 W and 461.57 W for brine solution, tofu whey and tuna cooking juice, respectively. Since tofu whey and tuna cooking juice contained higher salt and waste components than brine solution leading to decrease the vapor pressure and less vaporization on the membrane surface, in results less flux was obtained at high energy consumption [93, 94].

As the results shown in Figure 3.17 and Figure 3.18 can be seen that the permeate flux was increased with increasing feed temperature and as well as cross flow velocity. Otherwise, the value of EE (%) seems likely stable with increasing cross flow velocity. That can be concluding that the cross flow velocity is not effect on % EE.

It would clearly explained that the correlation between permeate flux and EE (%) was effected with feed temperature more than velocity. Martinez et al, 2001 [56] was studied the effect parameter on EE (%) in MD that the increase in heat of the cooling water is a sum of the latent heat of evaporation and the conduction heat lost through the membrane from the feed to the cooling water, as result low EE (%) was obtained.

In comparison, the process of DCMD was obtained high efficiency approximately 99.98 % of waste removal and less energy consumption to conventional processes such nanofiltration (NF), and ultrafiltration (UF). Normally, NF and UF was employed pressure as a driving force in range 1 to 5 bar to operate [16, 102], while 0.2 bar was applied for DCMD. Even though, high rejection, DCMD need to improve the design their configuration and enhanced the surface properties for obtain the permeate flux equal to NF or UF.

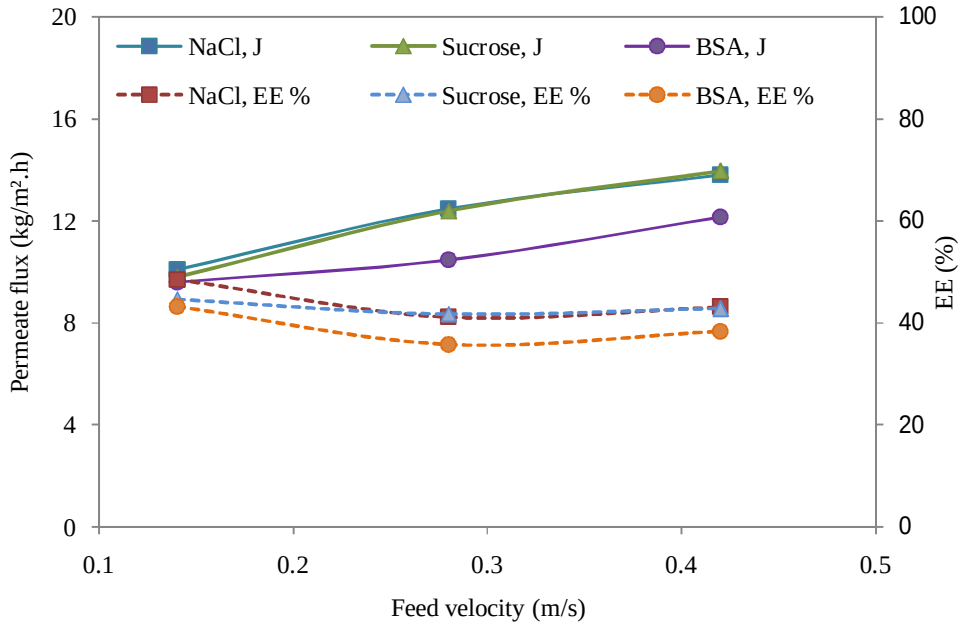

Figure 3.17 Permeate flux and evaporation efficiency EE (%) in function with velocity of synthesis solution; 3.5 wt.% 0f NaCl, 5 wt.% 0f sucrose, and 0.04 wt.% of BSA at feed temperature of 70 °C.

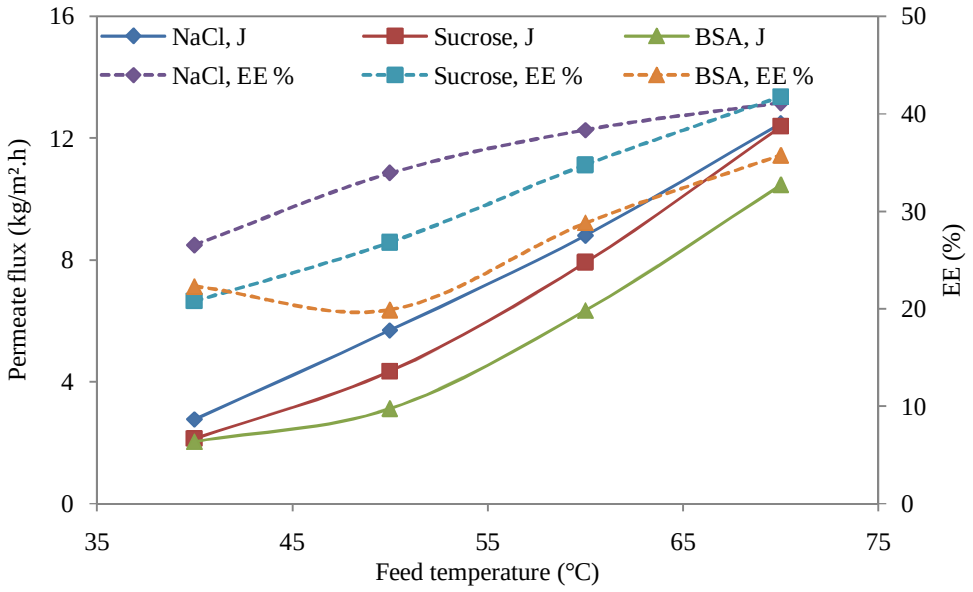

Figure 3.18 Permeate flux and evaporation efficiency EE (%) in function with feed temperature of synthesis solution; 3.5 wt.% of NaCl, 5 wt.% of Sucrose, and 0.04 wt.% of BSA at feed velocity of 0.28 m/s.

3.6 Gained output ratio

The cost of treatment process of food wastewater can be compared in terms of operational cost. Recently, energy consumption is the most challenges for MD treatment, which was estimated to be more than 450 kWh/m^3 compare to reverse osmosis is approximately 7 kWh/m^3, respectively [103, 104]. On the contrary, since MD depend upon only the temperature to generate the thermal driving force across the membrane, which enable to replace by waste heat or renewable solar energy to reduce the water production cost [103].

To measure the performance of thermal of the system, gained output ratio (GOR) was applied. The GOR is defined as the energy ratio of the latent heat of evaporation of the product water to the input thermal energy [105, 106]:

$$GOR = \frac{\Delta H_v m_{product}}{Q_{input}} \tag{3.7}$$

$$Q_{input} = m_h C_{pf}\left(T_{f,in} - T_{f,out}\right) \tag{3.8}$$

Where ΔH_v is the heat for water saturated vapor, $m_{product}$ is the water production, m_h is the feed flow rate, C_{pf} is the specific heat capacity of feed solution, and $T_{f,in}$ and $T_{f,out}$ are the feed inlet and outlet temperatures.

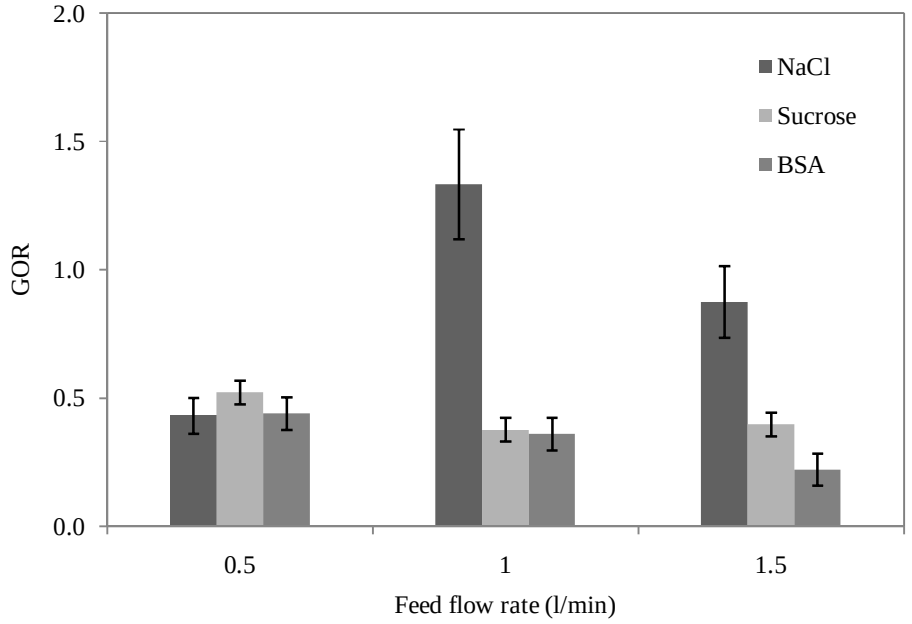

(a)

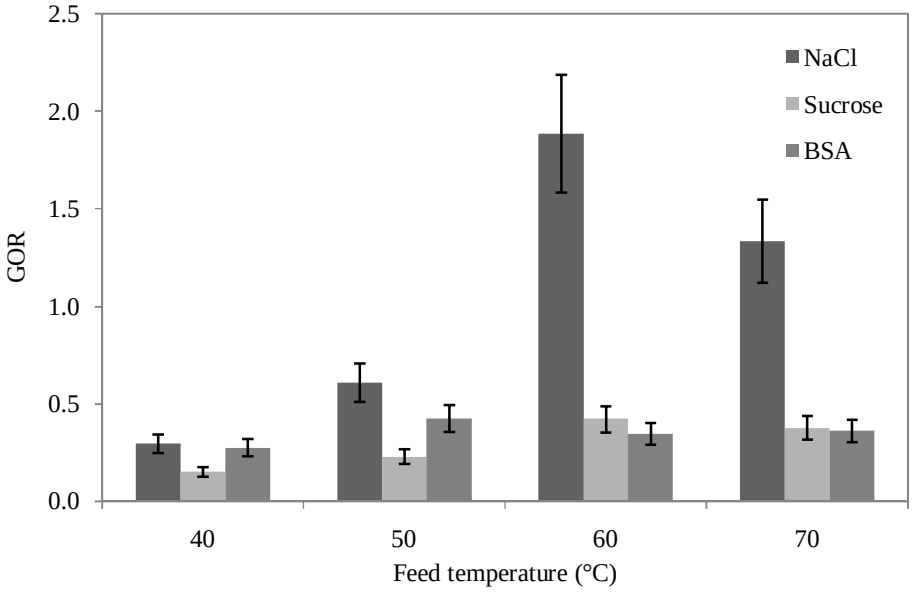

(b)

Figure 3.19 Energy consumption for the DCMD system under different operating conditions: (a) effect of flow rate (feed temperature: 70 °C and permeate temperature: 20 °C), and (b) effect of feed temperature (flow rate: 1 L/min and permeate temperature: 20 °C).

In the MD process, the energy consumption and GOR are important parameters. In Figure 3.19 shows the effect of feed temperature (a) and feed flow rate (b) on energy consumption and GOR ratio in different operating conditions. The GOR ratio was calculated to be in the range of 0.15 to 1.89 for three synthesis solutions. It can be seen that the optimized conditions to obtain the highest GOR of each solutions are steps as following:

- 3.5 wt.% of NaCl, the GOR reached 1.89 at feed temperature 60 °C with feed flow velocity of 0.28 m/s.
- 5 wt.% of sucrose, the GOR reached 0.52 at feed temperature 70 °C with feed flow velocity of 0.14 m/s.
- 0.04 wt.% of BSA, the GOR reached 0.44 at feed temperature 70 °C with feed flow velocity 0f 0.14 m/s.

In general, higher GOR in the systems represent more thermal energy efficiency were gained and consumed less energy. In review reported that GOR of membrane modules mostly has ranged from 0.3 to 6 (106-2100 kWh/m^3) [107-109].

Chapter 4
Conclusion and further works

The direct contact membrane distillation (DCMD) process in this study was applied in two steps. First, the DCMD was applied on synthesis solutions (3.5 wt.% of NaCl, 5 wt.% of sucrose and 0.04 wt.% of BSA) to study the effect of operating condition on permeate flux. The optimum conditions of feed temperature at 70 °C with flow velocity of 0.28 m/s were found to be appropriated for next step process. Second, using the optimize condition apply on real wastewater (brine solution, tofu whey and tuna cooking juice) to recover valuable compounds such as protein, sucrose as well as water production. All results can be indicated that highly temperature and velocity obtain higher permeate flux. The flux increases with an increasing in feed temperature difference ($\Delta T=50$), but decreases with an increasing in NaCl and protein concentration. The flux increases with flow rate, but permeate flux limited eventually causes a plateau. The maximum permeate flux value of a 0.1 μm PVDF membrane was observed to be 12.80, 10.59, 5.62 $kg/m^2.h$ for brine solution, tofu whey and tuna cooking juice, respectively. The minimum salt concentration and protein would be limited the system at 4,5 g/l and 2,5 g/l, respectively.

The percent rejection of waste characteristics was reached 99.98 % which enable to discharge free to water source or recycle used. Moreover, 26.21% and 32.53 % of sucrose and as well as protein concentration recovery from tofu whey and tuna cooking juice were achieved.

The energy efficiency is quite average, the high value obtained for the relative heat lost suggest that this system can be competitive only in situations where some source of waste energy is available. The increasing temperature is more significant effect on the energy efficiency than cross flow velocity.

The optimized conditions to obtain the highest GOR of each solution are steps as following:

- 3.5 wt.% of NaCl, the GOR reached 1.89 at feed temperature 60 °C with feed flow velocity of 0.28 m/s.
- 5 wt.% of sucrose, the GOR reached 0.52 at feed temperature 70 °C with feed flow velocity of 0.14 m/s.
- 0.04 wt.% of BSA, the GOR reached 0.44 at feed temperature 70 °C with feed flow velocity 0f 0.14 m/s.

In general, higher GOR in the systems represents the more thermal energy efficiency were gained and consumed less energy. In review reported that GOR of membrane modules mostly has ranged from 0.3 to 6 (106-2100 kWh/m^3).

For the further study are going to develop the configuration and modify the surface properties for enhance flux and maintain the less energy consumption.

REFERENCES

[1] National food institute 2009, Available: http://www.nfi.or.th/statistic.asp.

[2] Uttamangkabovorna, M., Prasertsan, P., Kittikun, A., 2005. Water conservation in canned tuna (pet food) plant in Thailand. Journalof Cleaner Production,13, (547-555).

[3] Nene, S., Kaurb, S., Sumodb, K., Joshib, B., Raghavarao, K.S.M.S. 2002. Membrane distillation for the concentration of raw cane-sugarsyrup and membrane clarified sugarcane juice Desalination 147(157-160).

[4] Adler-Nissen, J. Chapter 1: Introduction. Enzymatic Hydroliysis of food protein. Elsevier Applied Science Publishers, Essex. 1986; 1-21

[5] Lin, T.M., Park, J.W., Morrissey, M.T. 1995. Recovered protein and reconditioned water from surimi processing waste. J. Food Sci. 60: 4-9.

[6] Jaswal, A.S. 1990. Amino acid hydrolysis from crab processing waste. J. Food Sci. 55: 379-380, 397.

[7] Fonkwe, L.G., Singh, R.K. 1996. Protein recovery from mechanically deboned turkey residue by enzymatic hydrolysis. Process Biochem. 31, 605-616.

[8] Hoyle, N.T., Merritt, J.H. 1994. Quality of fish protein hydrolysates from herring. J. Food Sci. 59, 76-79, 129.

[9] Gunko, S., Verbych, S., Bryk, M., Hilal, N., 2006. Concnetration of apple juice using direct contact membrane distillation. Desalination.190, (117-124).

[10] Koz_ak, A., B_ek_assy-Moln_ar, E., Vatai, G. 2009. roduction of black_currant juice concentration by using membrane distllation. Desalination241, 309-314

[11] Nene, S., Kaurb, S., Umodb, K., Joshib, B., Raghavarao, K.M.S.M. 2002. Membrane distillation for the concentration of raw cane sugar-syrup andmembrane clarified sugarcane juice Desalination,147, (157-160).

[12] Christensen, K., Andresen, R., Tandskov, I., Norddahl, B., du Preez, J.H. 2006. Using direct contact membrane distillation for whey protein concentration. Desalination, 200(1–3), 523-525.

[13] Hausmann, A., Peter, S., Todor, V., Elankovan, P., Nohemi, Q.-C., Mike, W., Mikel, D. 2011. Direct Contact Membrane Distillation of Dairy Process Streams, 48-58.

[14] Qtaishat, M., Banat, F. 2013. Desalination by solar powered membrane distillation systems, Desalination.

[15] Song, L., Li, B., Sirkar, K.K., Gilron, J.L. 2007. Direct contact membrane distillation-based desalination: Novel membranes, devices, larger-scale studies, and a model. Ind. Eng. Chem. Res. 46, (2307–2323).

[16] Maria. D., Afonso, Rodrigo B., 2002. Review of the treatment of seafood processing wastewaters and recovery of proteins therein by membrane separation processes - prospects of the ultrafiltration of wastewaters from the fish meal industry. Desalination 142 (29-45).

[17] Singh, D., Sirkar, K.K. 2012. Desalination of brine and produced water by direct contact membrane distillation at high temperatures and pressures. Journal of Membrane Science 389, 380–388.

[18] Li, J., Guan, Y., Cheng, F., Liu, Y. 2015. Treatment of high salinity brines by direct contact membrane distillation: Effect of membrane characteristics and salinity.

[19] Ng, H.Y., Lee, L.Y., Ong, S.L., Tao, G., Viawanath, B., Kekre, K., Lay, W., Seah, H. 2008. Treatment of RO brine–towards sustainable water. Water Science & Technolgy- WST, 58.4.

[20] Lew, C. H., Hu, J. Y., Song, L. F., Lee, L. Y., Ong, S. L., Ng, W. J., Seah, H. 2005 Development of an integrated membrane process for water reclamation. Water Sci. Technol. 51(6–7), 455–463.

[21] Muschal, M. 2006. Assessment of risk to aquatic biotic from elevated salinity-A case study from the Hunter River, Austrialia. Journal of Environmenttal Management 79.3: 266-277.

[22] Jebamani, I.S., Gopalakrishnan, V., Senthilkumar, G. 2009. Brine solution recovery using nanofiltration.

[23] Jiang, C.X., Wang, Y.M., Zhang, Z.H., Xu, T.W. 2014. Electrodialysis of concentrated brine from RO plant to produce coarse salt and freshwater. Journal of Membrane Science 450, 323–330.

[24] Mericq, J.P., Laborie, S., Cabassud, C. 2010. Vacuum membrane distillation of seawater reverse osmosis brines. water research 44, 5260 -5273

[25] Thi, L.N., Champagne, C.P., Lee, B.H., Goulet, J.2003. Growth of Lactobacillus paracasei ssp. paracasei on tofu whey. International Journal of Food Microbiology 89, 67 – 75

[26] Ghofar, A., Ogawa, S., & Kokugan, T. 2005. Production of L-Lactic acid from fresh cassava roots slurried with tofu liquid waste by Streptococcus bovis. Journal of Bioscience and Bioengineering, 100, 606-612.

[27] Chang, K., Lin, Y.-S., & Chen, R. 2003. The effect of chitosan on the gel properties of tofu (soybean curd). Journal of Food Engineering, 57, 315–319.

[28] Lee, C.-Y., & Kuo, M.-I. 2011. Effect of c-polyglutamate on the rheological properties and microstructure of tofu. Food Hydrocolloids, 25, 1034–1040.

[29] Khatib, K.A., Aramouni, F.M., Herald, T.J., Boyer, J.E. 2001. Physicochemical characteristics of soft tofu formulated from selected soybean varieties.

[30] Chen, H., Jun, L.L., Jun, Z.J., Bo, X. and Rui, L. 2010. Chemical composition analysis of soybean oligosaccharides and its effect on ATPase activities in hyperlipidemics rats. Int. J. Biol. Macromol. 46:229-231.

[31] Atra, R., Vatai, G., Molnar, E.B. and Balint, A. 2005. Investigation of ultra- and nanofiltration for utilization of whey protein and lactose. J. Food Eng. 67:325-332.

[32] Uribe, B.C., Miranda, M.I.A., Costa, E.S., Roca, J.A.M., Clar, M.I.I. and Garcia, J.L. 2009. A study of the separation of lactose from whey ultrafiltration permeate using nanofiltration. Desalination. 241:244-255.

[33] Sakunda Anggarini, Nur Hidayat, Nimas Mayang Sabrina Sunyoto, Putri Siska Wulandari. 2015. Optimization of Hydraulic Retention Time (HRT) and Inoculums Addition in Wastewater Treatment Using Anaerobic Digestion System. Agriculture and Agricultural Science Procedia 3, 95 – 101.

[34] Heguang Zhu., Tomoo Suzuki., Anatoly A. Tsygankov., Yasuo Asada., Jun Miyake. 1999. Hydrogen production from tofu wastewater by Rhodobacter sphaeroides immobilized in agar gels. International Journal of Hydrogen Energy 24, 305-310.

[35] Zuofa Zhang, Guoying Lv, Huijuan Pan, Ashok Pandey, Weiqiang He, Leifa Fan. 2012. Antioxidant and hepatoprotective potential of endo-polysaccharides

from Hericium erinaceus grown on tofu whey. International Journal of Biological Macromolecules 51, 1140–1146.

[36] K. Seifert, M. Waligorska, M. Laniecki. 2010. Hydrogen generation in photobiological process from dairy wastewater. international journal of hydrogen energy 35, 9624-9629.

[37] Fithri Choirun Nisa, Hani R.H., Tri Wastono, B. Baskoro, Moestijanto. 2001. Produksi nata dari limbah cair tahu (whey): kajian penambahan sukrosa dan ekstrak kecambah. Jurnal Teknologi Pertanian, vol. 2, No. 2, August: 74-78.

[38] Kasiwut, J. 2012. Antioxidative, Angiotensin I-Converting Enzyme (ACE) Inhibitory and Ca-Binding Activities of Peptides Produced from Tuna cooking juice and spleen Extract-Protease. Thesis book.

[39] H-Kittikun. 2003. Enrichment of n-3 polyunsaturated fatty acid in tuna oil. In international seminar: Effective Utilization of Marine Food Resources. Prince of Songkla University. Hat Yai. Thailand. 18 December 2003.

[40] Lee, S.H., Qian, Z.J. and Kim, S.K. 2010. Anovel Angiotensin I converting enzyme inhibitory peptide from tuna frame protein hydrolysate and its antihypertensive effect in spontaneous hypertensive rat. Food Chem. 118:96-102.

[41] Prasertsan, P., Wuttijumnong, P., Sophadora, P. and Choorit, W. 1988. Seafood processing industries within Songkla-Hat Yai region: the survey of basic data emphasis on wastes. Songklanakarin. J. Sci. Technol. 10: 447-451.

[42] Walha, K., Ben Amar, R., Bourseau, P. and Jaoue, P. 2009. Nanofiltration of concentrated and salted tuna cooking juices. Process saf. Environ. 87: 331-335.

[43] Sujarit, C. 1997. Cultivation of Yeast in Tuna cooking juice after protein and fat Separation. M.Sc. Biotechnology. University of Songklanakarin.

[44] Sarabok, A., and H. Kittikun, A. 1999. Enzymatic hydrolysis of tuna cooking juice for flavor sauce production. Songklanakarin J.Sci. Technol. 21: 491-500.

[45] Jatupornpipat, M. 1994. Optimization for Growth and pigment synthesis of Rhodocyclus gelatinosus R7 Cultivating in Tuna cooking juice. M.Sci. Biotechnology. University of Songklanakarin.

[46] Kitrunkrote, K., Maneerut, S., and Bourtoom, T. 2000. Development of High Protein Tuna Soup Production from Tuna cooking juice. In proceedings of Development an dEngineering. P. 1-53.

[47] Alklaibi, A.M.; Lior, N. Membrane-distillation desalination: Status and potential. *Desalination*

[48] Zhang, J.; Dow, N.; Duke, M.; Ostarcevic, E.; Li, J.-D.; Gray, S. Identification of material and physical features of membrane distillation membranes for high performance desalination. *J. Membr. Sci.* 2010, *349*, 295–303.

[49] Laganà, F., Barbieri, G., Drioli, E. 2000. Direct contact membrane distillation: modelling and concentration experiments. Journal of Membrane Science 166, 1–11.

[50] Pabby, A.K., Rizvi, S.S.H., Sastre, A.M., 2009. Handbook of Membrane Separations: Chemical, Pharmaceutical, Food, and Biotechnological Applications. CRC Press

[51] El-Bourawi, M.S., Ding, Z., Ma, R., Khayet, M. 2006. Review-A framework for better understanding membrane distillation separation process Journal of Membrane Science 285, 4–29.

[52] Izquierdo-Gil, M.A., Garcia-Payo, M.C., FernaÂndez-Pineda, C. 2000 Air gap membrane distillation of sucrose aqueous solutions Journal of Membrane Science 155, 291±307.

[53] Kullab, A., Liu, C., Martin, A. 2005. Solar desalination using membrane distallation —technical evaluation case study, International Solar Energy Society Conference, Orlando, FL, August 2005.

[54] Lawson, K.W. and Lloyd, D.R., 1997, “Membrane Distillation (Review)”, Journal of Membrane Science, Vol. 124, pp. 1-25.

[55] Martinez-Diez, L.; Florido-Diaz, F.J. Theoretical and experimental studies on desalination using membrane distillation. *Desalination* 2001, *139*, 373–379.

[56] Martinez-Diez, L.; Florido-Diaz, F.J.; Vazquez-Gonzalez, M.I. Study of evaporation efficiency in membrane distillation. *Desalination* 1999, *126*, 193–198.

[57] Phattaranawik, J.; Jiraratananon, R. Direct contact membrane distillation: Effect of mass transfer on heat transfer. *J. Membr. Sci.* 2001, *188*, 137–143.

[58] Calabro, V.; Jiao, B.L.; Drioli, E. 1994. Theoretical and experimental study on membrane distillation in the concentration of orange juice. Ind. Eng. Chem. Res. 33, 1803–1808.

[59] Lawson, K.W.; Lloyd, D.R. Membrane distillation. I. Module design and performance evaluation using vacuum membrane distillation. *J. Membr. Sci.* 1996, *120*, 111–121.

[60] Garcia-Payo, M.C.; Rivier, C.A.; Marison, I.W.; von Stockar, U. Separation of binary mixtures by thermostatic sweeping gas membrane distillation: II. Experimental results with aqueous formic acid solutions. *J. Membr. Sci.* 2002, 198, 197–210.

[61] Basini, L.; D'Angelo, G.; Gobbi, M.; Sarti, G.C.; Gostoli, C. 1987. A desalination process through sweeping gas membrane distillation. *Desalination*, *64*, 245–257.

[62] Khayet, M.; Godino, P.; Mengual, J.I. 2000. Theory and experiments on sweeping gas membrane distillation. *J. Membr. Sci. 165*, 261–272.

[63] Khayet, M.; Godino, P.; Mengual, J.I. 2000. Nature of flow on sweeping gas membrane distillation. *J. Membr. Sci. 170*, 243–255.

[64] Rivier, C.A.; Garcia-Payo, M.C.; Marison, I.W.; von Stockar, U. 2002. Separation of binary mixtures by thermostatic sweeping gas membrane distillation: I. Theory and simulations. *J. Membr. Sci. 201*, 1–16.

[65] Josson, A.S.; Wimmerstedt, R.; Harrysson, A.C. 1985. Membrane distillation—A theoretical study of evaporation through microporous membranes. *Desalination 56*, 237–249.

[66] Bandini, S.; Gostoli, C.; Sarti, G.C. 1992. Separation efficiency in vacuum membrane distillation. *J. Membr. Sci. 73*, 217–229.

[67] Sarti, G.C.; Gostoli, C.; Bandini, S. 1993. Extraction of organic components from aqueous streams by vacuum membrane distillation. *J. Membr. Sci. 80*, 21–33.

[68] Cath, T.Y., Adams, D., Childress, A.E. 2004. Membrane contactor processes for wastewater reclamation in space II. Combined direct osmosis, osmotic distillation, and membrane distillation for treatment of metabolic wastewater. Journal of Membrane Science 257, 111.

[69] Khayet, M., Matsuura, T., 2011. Membrane Distillation: Principles and Applications. Elsevier, Amsterdam, Netherlands.

[70] Bui, V.A., Vu, L.T.T., Nguyen, M.H. 2010. Modelling the simultaneous heat and mass transfer of direct contact membrane distillation in hollow fibre modules. Journal of Membrane Science 353, 85–93.

[71] Khayet, M., 2011. Membranes and theoretical modeling of membrane distillation: a review. Adv. Coll. Interf. Sci. 164, 56–88.

[72] Qtaishat, M., Matsuura, T., Kruczek, B., Khayet, M., 2008. Heat and mass transfer analysis in direct contact membrane distillation. Desalination 219, 272–292.

[73] Bahmanyar, A., Asghari., M, Khoobi., N. 2012. Numerical simulation and theoretical study on simultaneously effects of operating parameters in direct contact membrane distillation. Chemical Engineering and Processing, 61, 42-50.

[74] Khayet, M., Mengual, J.I., 2004. Effect of salt concentration during the treatment of humic acid solutions by membrane distillation Desalination 168 (2004) 373-381.

[75] Martínez, L; Florido-Díaz, F.J. 2000. Theoretical and experimental studies on desalination using membrane distillation‖ Desalination 139 (2001) 373-379.

[76] M.R. Qtaishat, Use of vaccum membrane distillation for concentrating sugars and dyes from their aqueous solution, M.Sc. Thesis, Jordan university of Science and Technology, Jordan, 2004.

[77] Schofield, R.w., Fane, A.G., Fell, C.j. 1987. Heat and mass transfer in membrane distillation, Journal of Membrane Science. 33, 299-313

[78] Tomaszewska, M., Gryta, M., Morawski, A.W. 1992. Study on concentration of acids by membrane distillation, Journal of Membrane Science 102 113-122.

[79] Gryta, M. 2008. Fouling in direct contact membrane distillation process. J. Membr. 325, (1) 383-394

[80] Yang, X., Wang, R., Shi, L., Athonoy, G.F., Debowski, M. 2011. Performance improvement of follow fiber-based membrane distillation process. J. Membr. Sci. 369, 437-447.

[81] Lowry, O.H., Rosebrough, N.J., Farr, A.L., and Randall, R.J. 1951. Protein measurement with folin phenol reagent. J.Biol.Chem 193, 256-257.

[82] Wilson, K and Walker, J., 2000, Practical Biochemistry: Principles and Technique, CambridgeUniversity Press.

[83] Rice, E.W., Baird, R.B., Eaton, A.D., Clesceri, L.S., 2012. Standard Methods for the Examination of Water and Wastewater, (22nd Ed.). American Public Health Association, American Water Works Association, Water Environment Federation, USA.

[84] Bird M.R, Barlett M, 1995. Trans Inst Chem Eng [J], 73: 63-70.]

[85] Crowford J.G, Stober S.R, 1995. Preparation of soluble chymosin or prochymosin from recombinant E. Coli by solubilizing with urea and renaturing, with removal of urea by ultrafiltration for recycle and specific membrane cleaning procedure.

[86] Martinez-DõÂez, L., Vazquez-Gonzalez, M.I. 1999. Temperature and concentration polarization in membranedistillation of aqueous salt solutions. J.Sci, 156 (265-273)

[87] Veerman, C., Sagis, L.M.C., Heck, J., Van der Linden, E., 2003, Mesostructure of fibrillar bovine serum albumin gels. Int. J. Bio. Macromol., (139-146).

[88] Schofield, R.W., Fane, A.G., Fell, C.D.J. 1990. Factors affecting flux inmembrane distillation, Desalination 77, 279.

[89] Holman, J.P. 1986. Heat Transfer, sixth ed., McGraw-Hill, New York, NY.

[90] Kays, W.M., Crawford, M.E. 1993. Convective Heat and Mass Transfer,third ed., McGraw-Hill, New York, NY.

[91] Hoek, E.M., Bhattachajee, S., Elimelech, M. 2003. Effect of membrane surface roughness on colloid-membrane DLVO interactions. Langmuir 19, 4836-4847.

[92] Ding, Y., Tian, Y., Li, Z., Wang, H., Chen, L. 2013. Microfiltration (MF) membrane fouling potential evalution of protein with different ion strengths and divalent cations based on extended DLVO theory. Desalination, 331, 62-68.

[93] Zhang, J., Li, J.-D., Gray, S. 2011. Effect of applied pressure on performance of PTFE membrane in DCMD, J. Membr. Sci. 369, 514–525.

[94] He, K., Hwang, H.J., Woo, M.W., Moon, I.S. 2011. Production of drinking water from saline water by direct contact membrane distillation (DCMD) Journal of Industrial and Engineering Chemistry 17, 41–48.

[95] Gryta, M. 2007. Influence of polypropylene membrane surface porosity on the performance of membrane distillation process. J. Membr. Sci. 287(1) 67–78.

[96] He, F., Gilron, J., Lee, H., Song, L., Sirkar, K.K. 2008. Potential for scaling by sparingly soluble salts in crossflow DCMD, J. Membr. Sci. 311(1–2), 68–80.

[97] Hausmann, A., Sanciolo, P., Vasiljevic,T., Weeks, M., Schroën, K., Gray, S., Duke, M. 2013. Fouling of dairy components on hydrophobic polytetrafluoroethylene (PTFE) membranes for membrane distillation. Journal of Membrane Science 442, 149–159

[98] Cheryan, M. 1998. Ultrafiltration and Microfiltration Handbook, Technomic Pub, Lancaster.

[99] Ramachandra Rao, H.G. 2002. Mechanisms of flux decline during ultrafiltration of dairy products and influence of pH on flux rates of whey and buttermilk, Desalination 319–324144, 319–324.

[100] Kuberkar, V.T., Davis. R.H. 2001. Microfiltration of protein-cell mixtures with crossflushing or backflushing. Journal of Membrane Science 183, 1–14.

[101] Martinez-Diez, L., Florido-Diaz, F.J., V~quez-GonzS.lez., M.I. 1999. Study of evaporation efficiency in membrane distillation, Desalination 126 (193-198).

[102] Maria, D., Afonso., Rodrigo, B. 2002 Nanofiltration of wastewaters from the fish meal industry. Desalination 151 (131-138).

[103] Zuo, G., Wang, R., Field, R., Fane, A.G. 2011. Energy efficiency evaluation and economic analyses of direct contact membrane distillation system using Aspen Plus, Desalination 283, 237–244.

[104] Khayet, M., Godino, M.P., Mengual, J.I. 2003. Possibility of nuclear desalination through various membrane distillation configurations: a comparative study, Int. J. Nucl. Desalin. 1, 30–46.

[105] Koschikowski, J., Wieghaus, M., Rommel, M. 2003. Solar thermal-driven desalination plants based on membrane distillation. Desalination 156, 295–304.

[106] Wang, G.S., Ke, H., Gray, S., Il, S.M. 2015. Solar energy assisted direct contact membrane distillation (DCMD) process for seawater desalination. Separation and Purification Technology 143 94–104.

[107] Banat, F., Jwaied, N. 2007. Performance evaluation of the ‘‘large SMADES’’ autonomous desalination solar-driven membrane distillation plant in Aqaba, Jordan. Desalination 217, 17–28.

[108] Banat, F., Jwaied, N. 2007. Desalination by a ‘‘compact SMADES’’ autonomous solar powered membrane distillation unit, Desalination 217, 29–37.

[109] Fath, H.E., Elsherbiny, S.M., Hassan, A.A., Rommel, M., Wieghaus, M., Koschikowski, J., Vatansever, M. 2008. PV and thermally driven small-scale, stand alone solar desalination system with very low maintenance needs, Desalination 225 (1–3), 58–69.

APPENDIX A

Protein concentration by Lowry method (Lowry et al., 1951)

Apparatus

Spectrometer

Flask

Beaker

Test tube

Reagents

1. BSA stock solution (1 mg/ml)
2. Analytical reagents
   (a) 50 ml of 2 % sodium carbonate mixed with 50 ml of 0.1N NaOH solution
   (b) 10 ml 0f 1.56 % copper sulphate solution mixed with 10 ml of 2.37% sodium potassium tartrate solution.
   (c) Prepare analytical reagents by mixing 2 ml of (b) with 100 ml of (a)
   (d) Folin- Ciocalteau reagent solution dilute with distilled water 1:1

Procedure

1. Different dilutions of BSA solutions are prepared by mixing stock BSA solution (1 mg/ ml) and water in the test tube as given in the table. The final volume in each of the test tubes is 5 ml. The BSA range is 0.05 to 1 mg/ ml.
2. From these different dilutions, pipette out 0.2 ml protein solution to different test tubes and add 2 ml of analytical reagent (c). Mix the solutions well and incubate at room temperature for 10 min.
3. Then add 0.2 ml of analytical reagent (d) to each tube and incubate for 30 min. Zero the colorimeter with blank and take the optical density (measure the absorbance) at 750 nm.
4. Plot the absorbance against protein concentration to get a standard calibration curve.
5. Check the absorbance of unknown sample and determine the concentration of the unknown sample using the standard curve plotted above.

Capillary viscometer (AOAC, 2012)

Apparatus

Capillary viscometer branch Schott 531-10

Procedure

1. Place the viscometer in thermostatic water bath and maintained the temperature at 25 °C.
2. Transfer a sample about 2 ml to the tube A.
3. Transfer the sample to the tube B by suction until the sample raise to point C, when the sample flowed down from the point D to E of the capillary tube then measure the flow time (t=0 to t=t) by using stop watch.
4. Follow the step 2 and 3 for triple.
5. Using the average time to calculate the viscosity.
6. Using the equation as expressed below,

$$\eta = Dkt$$

ŋ= Viscosity of solution

D= Thickness of solution (kg/m^3)

k= Viscometer constant 0.01 (mm^2/s)

t= flow time (s)

$$D = \frac{M}{V}$$

M= Mass of solution which get from weight the 2 ml of solution

V= Quantity of solution (m^3)

Refractometer (AOAC, 2012)

Apparatus

Hand-held refractometer model ATAGO. Master-PM (Brix 0.0~33.0%) purchased from Japan with tolerance ±0.03%.

Procedure

1. First, Calibrate equipment by using deionized water drop on the plate which the value indicate 0 value.
2. Drop the sample on the plate and read the value
3. Do the step for triple times for average value.

Total kjeldahl nitrogen (TKN) by Kjeldahl method (AWWA, 2012)

Procedure

1. Selection of sample volume and sample preparation: Place a measured volume of sample in an 800-mL kjeldahl flask. Select sample size from the following tabulation:

Organic Nitrogen in Sample mg/L	Sample Size mL
0-1	500
1-10	250
10-20	100
20-50	50.0
50-100	25.0

If necessary, dilute sample to 300 mL, neutralize to pH 7, and dechlorinate.

2. Ammonia removal: Add 25 mL borate buffer and then 6*N* NaOH until pH 9.5 is reached. Add a few glass beads or boiling chips such as Hengar Granules #12 and boil off 300 mL. If desired, distill this fraction and determine ammonia nitrogen. Alternately, if ammonia has been determined by the distillation method, use residue in distilling flask for organic nitrogen determination.
3. Digestion: Cool and add carefully 50 mL digestion reagent (or substitute 6.7 mL conc H_2SO_4, 6.7 g K_2SO_4, and 0.365 g $CuSO_4$) to distillation flask. Add a few glass beads and, after mixing, heat under a hood or with suitable ejection equipment to remove acid fumes. Boil briskly until the volume is greatly reduced (to about 25 to 50 mL) and copious white fumes are observed (fumes may be dark for samples high in organic matter). Then continue to digest for an additional 30 min. As digestion continues, colored or turbid samples will become transparent and pale green. After digestion, let cool, dilute to 300 mL with water, and mix. Tilt flask away from personnel and carefully add 50 mL

sodium hydroxide-thiosulfate reagent to form an alkaline layer at flask bottom. Connect flask to a steamed-out distillation apparatus and swirl flask to insure complete mixing. The pH of the solution should exceed 11.0.

4. Distillation: Distill and collect 200 mL distillate. Use 50 mL indicating boric acid as absorbent solution when ammonia is to be determined by titration. Use 50 mL 0.04*N* H_2SO_4 solution as absorbent for manual phenate or electrode methods. Extend tip of condenser well below level of absorbent solution and do not let temperature in condenser rise above 29°C. Lower collected distillate free of contact with condenser tip and continue distillation during last 1 or 2 min to cleanse condenser.
5. Final ammonia measurement: Use the titration, ammonia-selective electrode, manual phenate, or automated phenate method.
6. Standards: Carry a reagent blank and standards through all steps of the procedure.

Biochemical Oxygen Demand (BOD) by standard method, 5210 B (AWWA, 2012)

Procedure

1. Determine the amount of sample to be analyzed; if available; use the historical results of a previous test of BOD_5 for a particular sampling site.
2. Place a clean, calibrated thermometer into the constant temperature chamber.
3. Turn on the constant temperature chamber to allow the controlled temperature to stabilize at 20°C ±1°C.
4. Turn on the DO instrument, but not the stirring attachment. Some DO instruments need to be turned on 30 to 60 minutes before calibration.
5. Aerate dilution water before adding nutrient solutions.
6. After aeration,

   a. Add to dilution water

   • 1 mL each of the potassium phosphate, magnesium sulfate, calcium chloride, and ferric chloride solutions per 1 L of dilution water, or

   • Hach Company nutrient buffer pillows to a selected volume of dilution water per the manufacturer's recommendation.

b. Shake the container of dilution water for about 1 minute to dissolve the slurry and to saturate the water with oxygen.

c. Place the dilution water in the constant temperature chamber to maintain a temperature of 20℃ until sample dilutions and analyses begin.

d. The initial and final (after 5 days ± 4 hours) DO tests of the dilution water is determined and recorded simultaneously with each batch of environmental samples.

7. Check the temperature of the air incubator or water bath using a laboratory thermometer to ensure that the temperature has been maintained at 20° ± 1℃. A minimum/maximum recording thermometer can be used to audit the temperature during times when checks cannot be made.
8. Place the sample container in the constant-temperature chamber or water bath to begin warming the sample to 20℃ ± 1℃. While the sample is warming, insert the air diffusion stone into the container and aerate the sample for about 15 minutes. After removing the air diffusion stone, allow several minutes for excess air bubbles to dissipate. The initial DO of the BOD sample needs to be at or slightly below saturation.

Calculation

The general equation for the determination of a BOD_5 value is:

$$BOD_5 \text{ (mg/L)} = \frac{D_1 - D_2}{P}$$

Where D_1 = initial DO of the sample,

D_2 = final DO of the sample after 5 days, and

P = decimal volumetric fraction of sample used.

Chemical Oxygen Demand (COD) by standard method, 5220 C (AWWA, 2012)

Procedure

1. Turn on the COD Reactor and preheat to 150 °C.
2. Homogenize 100 ml of sample for 30 seconds in a blender.
3. Remove the cap of a COD reagent vial and transfer the appropriate amount of sample into the vial. The dichromate ultra low range, low range, and high range COD products require 2.00 mL of sample. The dichromate high range plus COD requires 0.20 mL and the Manganese III COD reagent uses 0.50 mL of sample.
4. Replace the vial cap tightly. Hold the vial by the cap and invert several times over a sink to mix.
5. Place the vials into the pre-heated COD Reactor. Heat the vials for 1 hour (Mn III COD Reagent) or 2 hours (Dichromate COD Reagents).
6. Remove the vials from the reactor and cool to room temperature.

Total Alkalinity by titration method (AWWA, 2012)

Procedure

1. Using a clean sample bottle, collect sufficient sample from the water source to perform the required analyses; measure alkalinity within 24 hrs. Label each sample bottle using the date and related study identifier.
2. Before using the 01system, check the resistance on the digital readout of the system. Record resistance as required. Standard resistance for Type II 01water is >1. If there is an error message on the screen, contact the maintenance department. Use a balance to weigh chemical for the reagent preparation. Accuracy of the balance should be checked daily before use with a calibration weight set.
3. Prepare reagents as above (if needed).
4. Measure a 100 ml water sample into a 250 ml beaker. Set the sample on a magnetic stir plate with a stir bar.
5. Using a calibrated pH meter, begin titration with the sulfuric acid solution to an end point of pH 4.5. When nearing the end point, slow down the titration rate and be sure that pH equilibrium is reached before adding more titrant.
6. Calculate the total alkalinity and record.

Ash (AWWA, 2012)

Procedure

1. Heated the crucible in muffle furnace at 750 °C for 3 hours and left until temperature down in room temperature (30 °C), then putted into desiccators and weighed.
2. Repeated the heating for 30 minutes following as state on 1. Until its difference of weight less than 1-3 g.
3. A 2 g of sample was added into the crucible and heated in muffle furnace at 750 °C for 3 hours and repeated the method of 1 and 2.

Calculation

$$\%Ash = \frac{Weight\ of\ ash\ after\ heating}{Weight\ of\ ash\ before\ heating} \times 100$$

VITAE

Name Miss. Sothyreak Chhun

Student ID 5510120141

Educational Attachment

Degree	**Name of Institution**	**Year of Graduation**
Bachelor Rural Engineering	Institute of Technology of Cambodia	2012

Scholarship Awards during Enrolment

Scholarship provided by ASEA-UNINET (Asian European Academic University Network), and Thai higher education institution and Austrian Government (2012-2014).

List of proceeding

Sothyreak Chhun, Watsa Khongnakorn, Wirote Youravong, Effect of Operating Conditions of Direct Contact Membrane Distillation for Water Purification Proceeding: International Graduate Research Conference 2013 (iGRC 2013) 20, December 2013, Empress Hotel, Chiang Mai, Thailand.

List of Publications

Sothyreak Chhun, Watsa Khongnakorn, Wirote Youravong, Energy consumption for Brine solution recovery in Direct Contact Membrane Distillation. Advanced Materials Research Vols. 931-932 (2014) pp 256-260© (2014) Trans Tech Publications, Switzerland. doi:10.4028/www.scientific.net/AMR.931-932.256.